



**HAL**  
open science

## Strengthening the Connection between Science, Society and Environment to Develop Future French and European Bioeconomies: Cutting-Edge Research of VAALBIO Team at UCCS

Marcia Araque-Marin, Fabio Bellot Noronha, Mickäel Capron, Franck Dumeignil, Michèle Friend, Egon Heuson,IVALDO Itabaiana, Louise Jalowiecki-Duhamel, Benjamin Katryniok, Axel Löfberg, et al.

### ► To cite this version:

Marcia Araque-Marin, Fabio Bellot Noronha, Mickäel Capron, Franck Dumeignil, Michèle Friend, et al. Strengthening the Connection between Science, Society and Environment to Develop Future French and European Bioeconomies: Cutting-Edge Research of VAALBIO Team at UCCS. *Molecules*, 2022, 27 (12), pp.3889;. 10.3390/molecules27123889 . hal-03771396

**HAL Id: hal-03771396**

**<https://hal.science/hal-03771396>**

Submitted on 7 Sep 2022

**HAL** is a multi-disciplinary open access archive for the deposit and dissemination of scientific research documents, whether they are published or not. The documents may come from teaching and research institutions in France or abroad, or from public or private research centers.

L'archive ouverte pluridisciplinaire **HAL**, est destinée au dépôt et à la diffusion de documents scientifiques de niveau recherche, publiés ou non, émanant des établissements d'enseignement et de recherche français ou étrangers, des laboratoires publics ou privés.

Review

# Strengthening the Connection between Science, Society and Environment to Develop Future French and European Bioeconomies: Cutting-Edge Research of VAALBIO Team at UCCS

Marcia Araque-Marin <sup>1</sup>, Fabio Bellot Noronha <sup>1,2</sup> , Mick ael Capron <sup>1</sup> , Franck Dumeignil <sup>1</sup> , Mich ele Friend <sup>1,3</sup>, Egon Heuson <sup>1</sup> ,IVALDO Itabaiana, Jr. <sup>1,4</sup> , Louise Jalowiecki-Duhamel <sup>1</sup>, Benjamin Katryniok <sup>1,\*</sup>, Axel L ofberg <sup>1</sup> , S ebastien Paul <sup>1,\*</sup>  and Robert Wojcieszak <sup>1</sup>

- <sup>1</sup> Univ. Lille, CNRS, Centrale Lille, Univ. Artois, UMR 8181-UCCS-Unit  de Catalyse et Chimie du Solide, F-59000 Lille, France; marcia-carolina.araque-marin@centralelille.fr (M.A.-M.); fabio.bellot@int.gov.br (F.B.N.); mickael.capron@univ-lille.fr (M.C.); franck.dumeignil@univ-lille.fr (F.D.); michele@gwu.edu (M.F.); egon.heuson@centralelille.fr (E.H.); ivaldo@eq.ufrj.br (I.I.J.); louise.duhamel@univ-lille.fr (L.J.-D.); axel.lofberg@univ-lille.fr (A.L.); robert.wojcieszak@cnrs.fr (R.W.)
- <sup>2</sup> Catalysis, Biocatalysis and Chemical Processes Division, National Institute of Technology, Rio de Janeiro 20081-312, Brazil
- <sup>3</sup> Department of Philosophy, George Washington University, Washington, DC 20052, USA
- <sup>4</sup> Department of Biochemical Engineering, School of Chemistry, Federal University of Rio de Janeiro, Rio de Janeiro 21941-910, Brazil
- \* Correspondence: benjamin.katryniok@centralelille.fr (B.K.); sebastien.paul@centralelille.fr (S.P.)



**Citation:** Araque-Marin, M.; Bellot Noronha, F.; Capron, M.; Dumeignil, F.; Friend, M.; Heuson, E.; Itabaiana, I., Jr.; Jalowiecki-Duhamel, L.; Katryniok, B.; L ofberg, A.; et al. Strengthening the Connection between Science, Society and Environment to Develop Future French and European Bioeconomies: Cutting-Edge Research of VAALBIO Team at UCCS. *Molecules* **2022**, *27*, 3889. <https://doi.org/10.3390/molecules27123889>

Academic Editors: Pascal Isnard, Jerome Guillard, Franck Launay and Jean-Hugues Renault

Received: 26 May 2022

Accepted: 15 June 2022

Published: 17 June 2022

**Publisher's Note:** MDPI stays neutral with regard to jurisdictional claims in published maps and institutional affiliations.



**Copyright:**   2022 by the authors. Licensee MDPI, Basel, Switzerland. This article is an open access article distributed under the terms and conditions of the Creative Commons Attribution (CC BY) license (<https://creativecommons.org/licenses/by/4.0/>).

**Abstract:** The development of the future French and European bioeconomies will involve developing new green chemical processes in which catalytic transformations are key. The VAALBIO team (valorization of alkanes and biomass) of the UCCS laboratory (Unit  de Catalyse et Chimie du Solide) are working on various catalytic processes, either developing new catalysts and/or designing the whole catalytic processes. Our research is focused on both the fundamental and applied aspects of the processes. Through this review paper, we demonstrate the main topics developed by our team focusing mostly on oxygen- and hydrogen-related processes as well as on green hydrogen production and hybrid catalysis. The social impacts of the bioeconomy are also discussed applying the concept of the institutional compass.

**Keywords:** bioeconomy; catalysis; glycerol; furanics; hybrid catalysis; lignin; polymers

## 1. Introduction

Since its creation in 2006, the VAALBIO group, standing for valorization of alkanes and biomass, has constantly been conducting dynamic research at UCCS (Unit  de Catalyse et Chimie du Solide–UCCS UMR CNRS 8181), located in Lille, on catalysis for biomass valorization. This topic is indeed a pillar of bioeconomy development not only in France but also in Europe. The VAALBIO team today comprises more than 40 researchers. The group is internationally recognized in the field of heterogeneous catalysis and catalytic processes [1]. Recently, the VAALBIO team extended its research areas to chemo-enzymatic catalysis [2], hybrid catalysis and, even more recently, to human sciences [3] to be able to measure the impact of the implementation of new sustainable processes in future biorefineries. In this Special Issue of *Molecules* dedicated to “Sustainable Chemistry in France”, a few examples of our recent results are presented. For the sake of clarity, this review paper is divided based on the catalytic process. In the first part, the valorization of biosourced platform molecules such as alcohols, polyols or furanics using different atmospheres (oxidative, reductive, or neutral) is presented. In the second part, biomass fractionation and green hydrogen production are discussed. The combination of enzymatic catalysis and chemo-catalysis to

carry out hybrid catalysis may lead to a real breakthrough in the field of catalysis in the coming years. The most recent advances of our group in this field are detailed hereafter. Finally, the new concept of institutional compass, a tool to assess the impact of the new renewable processes is also presented.

## 2. Recent Works and Results

### 2.1. Reactions Involving Oxygen

#### 2.1.1. Selective Oxidation of Glycerol

Glycerol is a waste product of biodiesel production. It is obtained as a byproduct of the reaction of the transesterification of triglycerides, which yields biodiesel (ca. 1 kg of glycerol is produced per 9 kg of biodiesel). Glycerol is considered as an important platform molecule due to (i) its high potential, thanks to the presence of three hydroxyl groups, which provide a high reactivity, and (ii) numerous upgrading possibilities (various target molecules) [4]. Figure 1 presents some of the molecules of interest that can be produced from glycerol such as epichlorohydrin through halogenation (epichlorohydrin), to diols as monomers for subsequent polymerization through reduction, acrolein which is a synthon that can be used to produce feed (DL-methionine) or super-adsorbent polymers for diapers (acrylates) through dehydration, and a variety of aldehydes, ketones or carboxylic acids of interest through selective oxidation to.

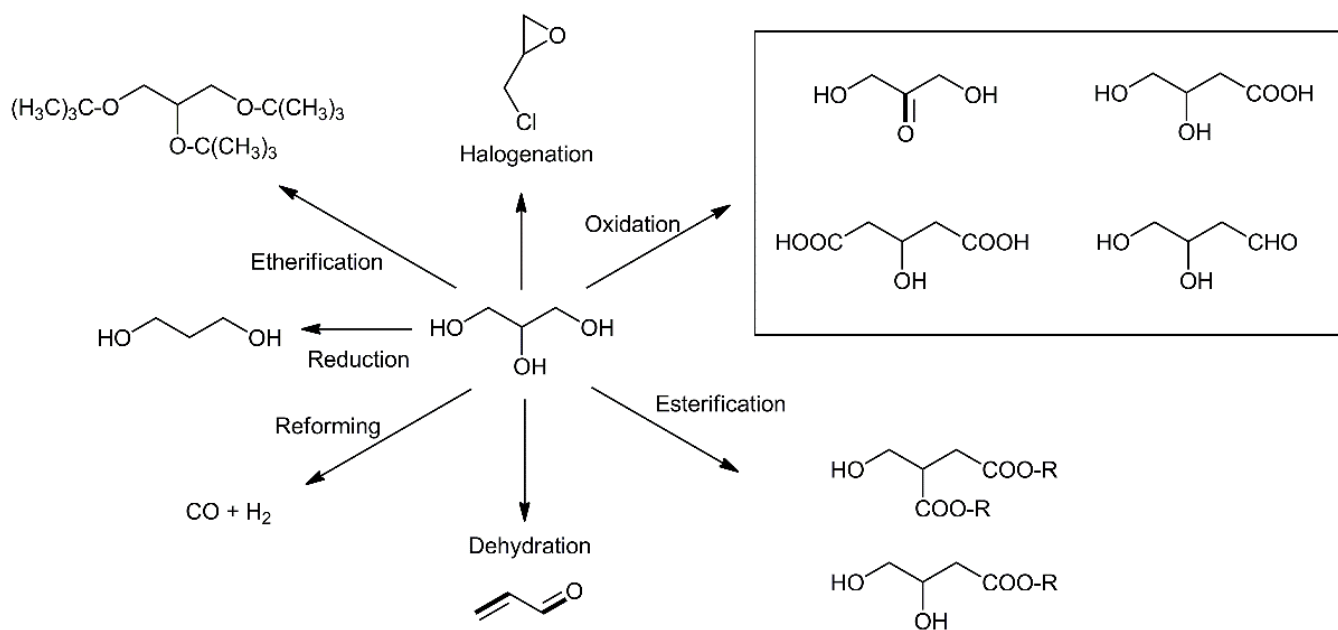


**Figure 1.** Examples of molecules of interest obtained through upgrading glycerol.

Among the aforementioned reactions, many studies have especially been published on the glycerol oxidation reaction in the liquid phase [5]. Most authors used noble metal-based catalysts (i.e., Pt, Au) in a basic medium to produce mainly glyceric and tartronic acids [6–9]. In our lab, mechanistic and kinetic studies have been carried out to compare the effects of various metals [10,11]. It has generally been observed that Au-based catalysts are only active in basic media, while Pt-based catalysts are more active and can be operated in a wide pH range (i.e., from basic to acid media). Because the price of glycerol strongly depends on its purity, we studied the effect of the different impurities present in crude glycerol [8]. The conclusion of such a study is that “impurities” such as methanol or the base used during the transesterification process help the oxidation of glycerol, but sulfides and MONG (i.e., Matter Organic Non-Glycerol: triglycerides and free fatty acids) hinder the catalytic performances drastically, mainly in terms of glycerol conversion, while selectivity is not impacted. Thus, prior to a catalytic reaction, it is highly recommended to at least

remove MONG from crude glycerol, as it induces a strong deactivation of most catalysts by physically blocking their access to the active sites.

In the literature, only a few studies focusing on the production of glyceraldehyde from glycerol have been carried out [12–14], even though this aldehyde could be applied in many sectors (e.g., pharmaceuticals, cosmetics, etc.). Among the conventional metals used for glycerol oxidation in the liquid phase, only Pt shows a good activity toward glyceraldehyde formation. We performed our first study [15] on Pt/Al<sub>2</sub>O<sub>3</sub> prepared using various methods, leading to various Pt nanoparticles sizes. We evidenced that in base-free conditions (but also in basic ones), selectivity is glycerol conversion dependent. Then, we dedicated a full study to the aforementioned reaction [16], keeping Pt as an active metal deposited on various supports and evidenced clearly that the selectivity toward glyceraldehyde is inversely linearly proportional to the glycerol conversion, irrespective of the support. Our lab-made Pt catalysts supported on SiO<sub>2</sub>, Al<sub>2</sub>O<sub>3</sub> or TiO<sub>2</sub> exhibited different initial glycerol conversion rates, highlighting them as good catalysts for the production of glyceraldehyde (i.e., Pt/TiO<sub>2</sub>). The Pt/TiO<sub>2</sub> catalyst presents the smallest initial conversion rate and also the highest glyceraldehyde selectivity.

Glycerol oxidation with C-C bond cleavage can lead to glycolic acid. This molecule finds applications as a tanning agent or in cosmetic formulations, for example. Only very few studies focus on the production of glycolic acid. This is due to the fact that over conventional noble metal-based catalysts under basic conditions, the formation of C3 acids is mainly observed (especially tartronic and glyceric acids). We demonstrated that by using Ag-based catalysts and choosing the ad hoc support, it is possible to favor the formation of glycolic acid [17,18]. Like for the aforementioned reaction, we first focused on a low glycerol concentration (i.e., 0.3 M) using a 1.4 wt.% Ag/Al<sub>2</sub>O<sub>3</sub> catalyst. We chose different types of Al<sub>2</sub>O<sub>3</sub> presenting different acid–basic characters (i.e., basic Al<sub>2</sub>O<sub>3</sub>, acidic Al<sub>2</sub>O<sub>3</sub> and  $\alpha$ -Al<sub>2</sub>O<sub>3</sub>). We showed that it is very important that the support presents a basic character in order to efficiently transform glycerol to glycolic acid. The evolution of glycolic acid yield follows the following order: basic Al<sub>2</sub>O<sub>3</sub> > acidic Al<sub>2</sub>O<sub>3</sub> >  $\alpha$ -Al<sub>2</sub>O<sub>3</sub> [18]. In order to optimize the catalyst formulation, we thus worked on different kinds of basic supports, keeping the other potential variables constant (e.g., the quantity of Ag, reaction conditions, etc.) [19]. As illustrated in Figure 2, the catalysts constituted of 1.4 wt.% Ag deposited on hydrotalcite (HPA) or on La<sub>2</sub>O<sub>3</sub>, well known for their basic characters, orientated the selectivity toward glyceric acid. In this figure, we can see that using ZrO<sub>2</sub> and CeO<sub>2</sub> allows us to increase the glycolic yield compared to the aforementioned basic alumina (first catalyst presented in Figure 2). The next step of the study was to prepare a new support by mixing the two aforementioned ones and increasing the quantity of silver [20], which led to an optimal composition, 5 wt.%/Ce<sub>0.75</sub>Zr<sub>0.25</sub>O<sub>2</sub>. Owing to this formulation, we worked on the optimization of glycolic acid productivity by increasing the initial glycerol concentration up to 2 M. Using a Design of Experiments (DOE) methodology, we thus optimized the reaction conditions in order to maximize glycolic acid productivity. We obtained 0.88 M of glycolic acid, starting from a 2 M glycerol solution. Increasing the initial glycerol conversion led to the need for an increase in O<sub>2</sub> in the batch reactor.

### 2.1.2. Allyl Alcohol Oxidation to Acrylic Acid

Acrylic acid is one of the most commonly used intermediates used today, with USD 12 billion being spent on it in 2020. The selective oxidation of allyl alcohol to acrylic acid was studied over orthorhombic, trigonal, tetragonal and amorphous Mo<sub>3</sub>VO<sub>x</sub> [21]. The orthorhombic and trigonal Mo<sub>3</sub>VO<sub>x</sub> catalysts showed very similar catalytic performances, with an interesting shift in selectivity depending on the reaction temperature. In fact, at low temperatures (<200 °C), propanal and acrolein were found as the main products. Upon increasing the reaction temperature, the selectivity of the latter decreased gradually, giving rise to acrylic acid and propionic acid and yielding up to 66% acrylic acid at 350 °C for the orthorhombic Mo<sub>3</sub>VO<sub>x</sub> catalyst and 68% at 325 °C for the trigonal Mo<sub>3</sub>VO<sub>x</sub> catalyst. On the other hand, the tetragonal Mo<sub>3</sub>VO<sub>x</sub> catalyst was much less active than

the orthorhombic  $\text{Mo}_3\text{VO}_x$  and trigonal  $\text{Mo}_3\text{VO}_x$  catalysts, and exhibited a totally different product distribution, mainly yielding acrolein (>70%), even at an increased reaction temperature of 400 °C. Since all the studied catalysts have the same chemical composition, the difference in the observed catalytic activity was ascribed to the structure, meaning that the reaction is structure sensitive. In fact,  $\text{Mo}_3\text{VO}_x$  possesses the same layer-type structure in the c-direction, but with a different arrangement of the pentagonal  $\{\text{Mo}_6\text{O}_{21}\}$  units in the a-b plane (Figure 3) [22]. Orthorhombic, trigonal and amorphous  $\text{Mo}_3\text{VO}_x$  exhibit heptagonal channels, whereas tetragonal  $\text{Mo}_3\text{VO}_x$  does not. The exposed section surface and the side surface of the rod-shaped crystals provide different active sites for oxidation reactions. Since the arrangement in the c-direction was identical for the four catalysts, it was concluded that the side surface of the  $\text{Mo}_3\text{VO}_x$  catalysts was responsible for the selective oxidation from allyl alcohol to acrolein, whereas the heptagonal arrangement in the a-b plane catalyzed the oxidation of allyl alcohol to acrylic acid. It is further worth pointing out that the catalysts exhibited stable performances throughout the whole catalytic test cycle (>72 h), evidencing the high stability of the structure and the absence of any sintering or phase rearrangement, also shown by the XRD and  $\text{N}_2$ -physisorption of the spent catalysts.

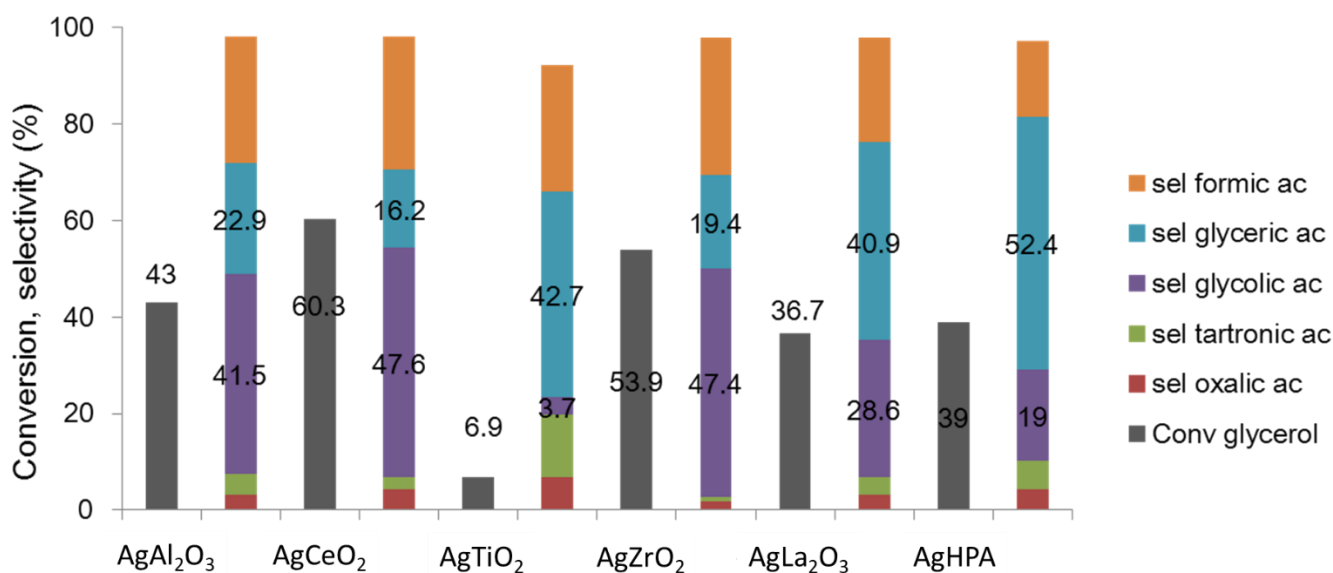


**Figure 2.** Glycerol oxidation using Ag-based catalysts. Reaction conditions: 5 h at 60 °C, 5 bar  $\text{O}_2$ ,  $\text{NaOH}/\text{GLY} = 4$  (molar ratio), 0.3 M glycerol, 0.5 g catalyst, 1.4 wt.% Ag/support, and batch reactor.

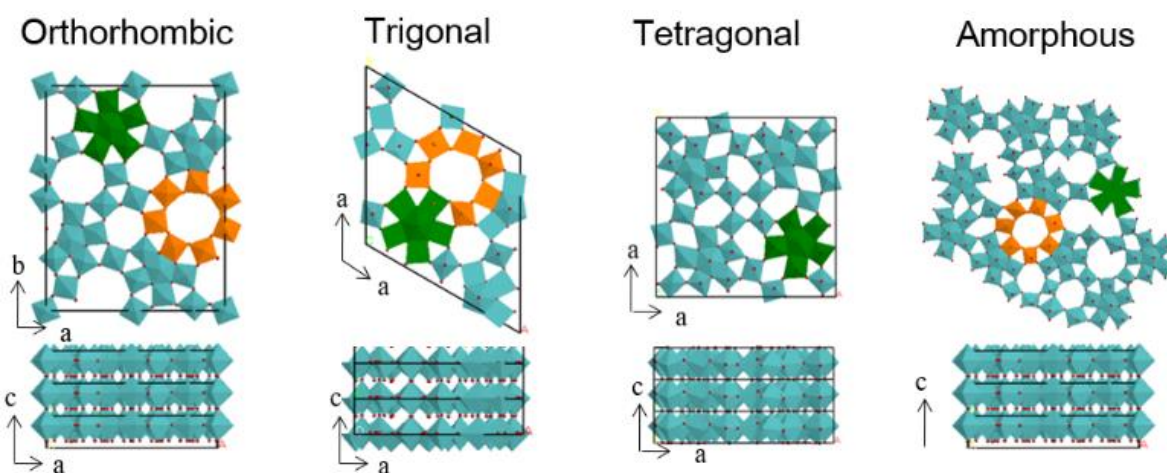


**Figure 3.** Structures of  $\text{Mo}_3\text{VO}_x$  catalysts employed in the selective oxidation of allyl alcohol to acrylic acid.

### 2.1.3. Selective Oxidation of Furanics

Chemically speaking, furfural and 5-hydroxymethylfurfural are heteroaromatic molecules (furan ring) that also contain an aldehyde group. The transformation of these molecules into valuable chemicals is made possible by the presence of these functional groups [23]. The aldehyde group can be oxidized to an acid or undergo direct oxidative esterification. Below, we discuss the most important aspects that bring together works from the recent years of research on the catalytic transformations of furfural (FF) and 5-hydroxymethylfurfural (HMF) through oxidation processes. Given that Au-based catalysts have shown a high potential for achieving the aerobic oxidation of many substrates in water, their use in furfural oxidation would be advantageous [23–25]. However, the use of gold catalysts for the production of furoic acid, maleic acid, or succinic acid under uncontrolled pH conditions (without the addition of a base) is not well documented yet. Some of the first documents on this topic were published by our group [26–35]. Over the last 10 years of research on furfural oxidation, we have studied several factors that influence conversion and selectivity in this process. All works were performed in base-free conditions. In addition, we have also developed an in situ method to monitor the liquid phase oxidation of furfural via Raman spectroscopy [34]. Our first study focused on gold nanoparticles supported on different hydrotalcites [27]. It is known that the basicity of a hydrotalcite carrier strongly depends on the Mg:Al ratio used during synthesis. Hydrotalcite supports were prepared by a co-precipitation method using different Mg:Al ratios (5:1, 4:1, 3:1 and 2:1). All catalysts were active in the liquid phase oxidation of furfural at 110 °C and under 6 bar of oxygen. As expected, strong increases both in the furfural conversion and the yield to furoic acid were observed using supported gold nanoparticles catalysts as compared to the supports alone [27]. All catalysts were active in the oxidation of furfural in the liquid phase at 110 °C and under 6 bar of oxygen (Table 1). As expected, strong increases in both furfural conversion and furoic acid yield were observed using gold nanoparticle catalysts compared to the supports alone [27].

**Table 1.** Comparison of furfural oxidation efficiency for Au/HT catalysts with supports of different Mg: Al molar ratios. Reaction:  $p = 6$  bar ( $O_2$ );  $t = 110$  °C; 2 h; 600 rpm; FF/Au molar ratio = 200:1; [FF] = 22.7 mM; 25 mg catalyst. Adapted with permission from Ref. [27].

Catalyst	Temperature (°C)	Conversion (%)	FA Selectivity (%)	Carbon Balance (%)
Au/HT 2:1	110	82	86	89
Au/HT 3:1	110	76	88	91
Au/HT 4:1	110	99	100	100
Au/HT 5:1	110	99	100	100

Complete conversion and 100% selectivity to furoic acid were achieved with Au/HT 4:1 and Au/HT 5:1 catalysts. This was probably due to the increase in the overall alkalinity of the support, which promoted the activity of the catalysts. No leaching of gold was detected; however, the Mg concentration in the post-reaction mixture steadily increased with reaction time, indicating gradual leaching. The pH of all samples after the reaction was 7, which was not expected since both furfural and furoic acid solutions have a pH of about 3 in water. This is strong evidence that a soluble base was formed in situ [27]. Our works showed that the presence of MgO is essential to achieve a high activity of the catalysts due to the in situ -OH formation. However, the dissolution of the support is an important issue. We tried to find a way to stabilize the MgO on the catalyst and to prevent the leaching. Thus, we proposed a novel catalyst in which Au is supported on a Mg-based support, a MgF<sub>2</sub>-MgO mixed phase solid [29]. Au/MgF<sub>2</sub> displayed a rather low catalytic activity, similar to those of titania-, zirconia- and ceria-based catalysts, although it was less prone to the formation of FA.

The presence of the catalyst did not yield any change in the reaction pH, so there was no evidence of support leaching. Therefore, the degradation and/or side reactions and lower catalytic performance can be attributed to the acidic reaction medium, which

does not favor Au-based solid catalytic functions. Decreasing the content of  $\text{MgF}_2$  in the mixed-phase ( $\text{MgF}_2\text{-MgO}$ ) support resulted in higher conversions, FA yields and carbon mass balances, as highlighted in Figure 4. Au/ $\text{MgF}_2\text{-MgO}$  catalysts were very effective in the oxidation of furfural to FA, reaching a 99% yield after 2 h of reaction. A value of 60 mol % of magnesium oxide in the mixed system ( $\text{MgF}_2\text{-MgO}$ ) is enough to provide the same activity as that of pure  $\text{MgO}$  under the same conditions [29].

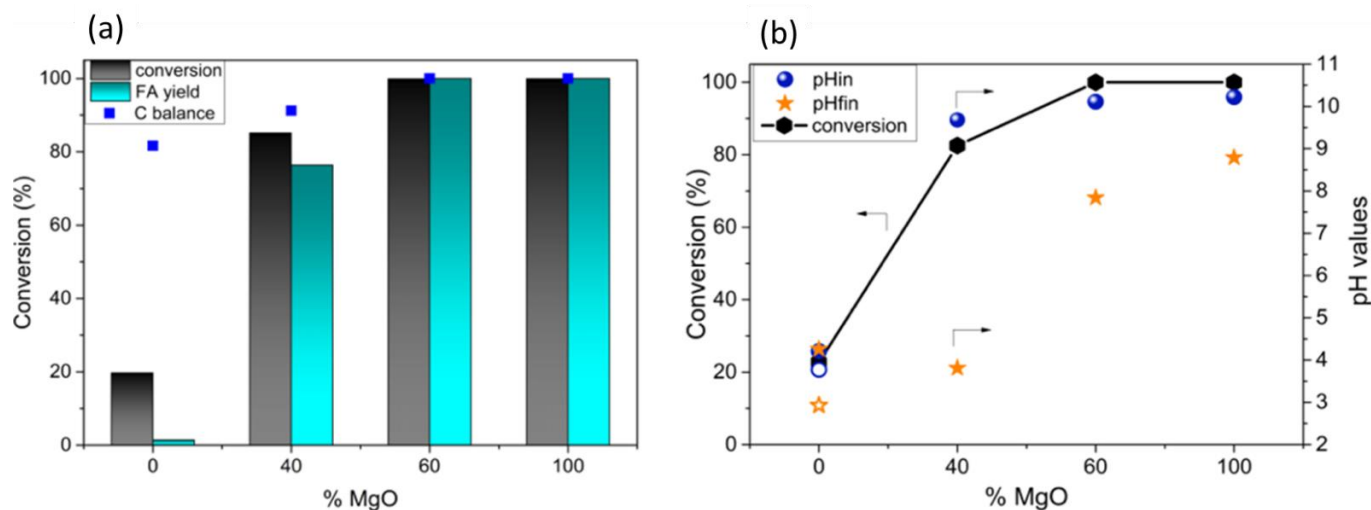


**Figure 4.** Base-free furfural oxidation using Au-based catalysts supported on the  $\text{MgF}_2\text{-MgO}$  with various relative amounts of  $\text{MgF}_2$  and  $\text{MgO}$ . (a) Furfural conversion and FA yield versus %  $\text{MgO}$ ; (b) furfural conversion and initial and final pH values versus %  $\text{MgO}$  (solid symbols) and blank test (open symbol) ( $49.4 \mu\text{mol}$ , substrate/metal = 50 (mol/mol), air (26 bar),  $110^\circ\text{C}$ , 600 rpm, 2 h).  $\text{pH}_{\text{in}}$  indicates the pH measured before reaction (furfural solution + catalyst) and  $\text{pH}_{\text{fin}}$  indicates the pH measured after reaction. Reprinted with permission from Ref. [29].

#### 2.1.4. Adipic Acid Synthesis

Adipic acid is one of the most important chemical intermediates—with a foreseen market of USD 8 billion in 2024—used in the preparation of nylon-6,6 polyamide, fibers and plasticizers. It is generally obtained using  $\text{HNO}_3$  in a two-step process. The oxidation process of cyclohexanone and cyclohexanol (KA oils) is seriously harmful to the environment because of the nitrous oxide ( $\text{N}_2\text{O}$ ) produced in huge amounts. It is generally thought to be a major factor of global warming and specifically of ozone depletion [36]. With this objective, we developed a new process which could be industrially applicable. The VAALBIO group is working on two different routes to obtain adipic acid. Cyclohexane was chosen as a starting reagent because it is largely available and not expensive.

Moreover, unlike to cyclohexene, it can be oxidized using air under solvent-free conditions. Produced adipic acid is not soluble in cyclohexane and can be easily removed from the reaction media (Figure 5a). The highest AA selectivity and yield in a 1 mol scale reaction was obtained at  $135^\circ\text{C}$  after 10 h of reaction using the VPO/ $\text{CeO}_2$  catalyst (Table 2).

Adipic acid can also be obtained through the oxidation of 1,6-hexanediol, as presented in Figure 5b. We have investigated this reaction using supported gold nanoparticles with different particle sizes and particle size distributions [37]. The mean diameters of the gold nanoparticles varied from 3 to 8 nm. Various experimental parameters were studied for the optimization of reaction conditions, such as the Au/HDO ratio, NaOH equivalent, agitation and temperature (Figure 6), by applying the DoE approach. We showed that the most important parameters are Au particle size, HDO to Au molar ratio and agitation. The best results in terms of the adipic acid yield were obtained using Au obtained via the sol-immobilization method with polyvinyl alcohol (PVA) catalysts (40% at  $110^\circ\text{C}$ ), however, with a low HDO to Au molar ratio (100). Under basic conditions and with a high

HDO to Au ratio, the adipic acid yield was about 20%, with a much higher carbon balance (about 95%) [37].

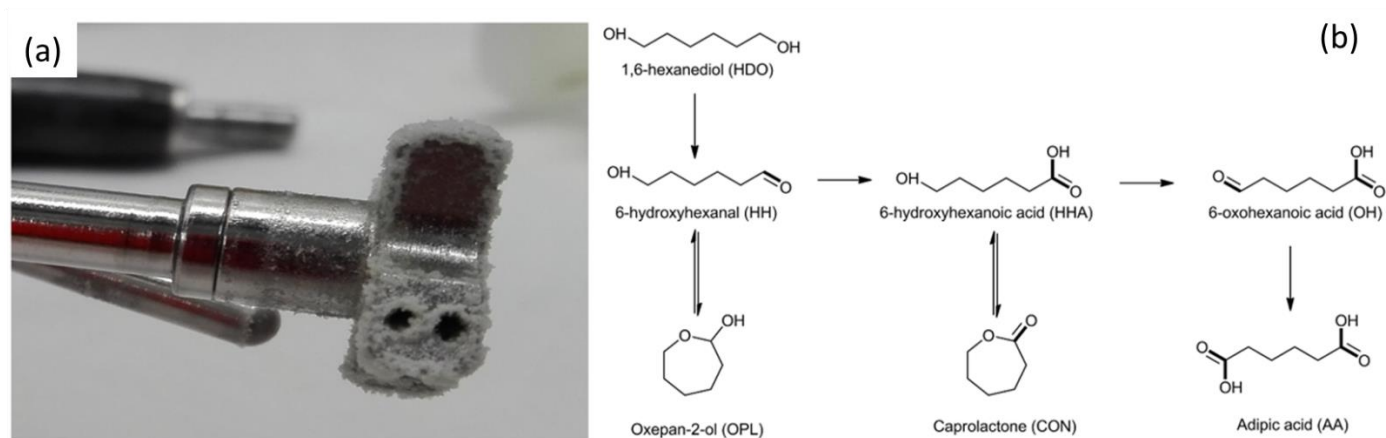


**Figure 5.** (a) Adipic acid formed from cyclohexane oxidation under solvent-free conditions; (b) adipic acid synthesis pathways from 1,6-hexanediol.

**Table 2.** Effect of the time of 1,6 hexanediol oxidation reaction at 120 °C and 135 °C. Adapted with permission from Ref [36].

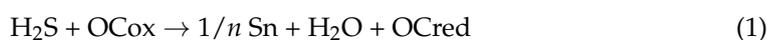
T <sup>a</sup> (°C)	t <sup>b</sup> (h)	X Cha <sup>c</sup> (%)	Selectivity <sup>d</sup> (%)				
			Chole	Chone	AA	GA	SA
120	4	1.2	84	11	5	0	0
	10	5.2	66	17	13	4	0
135	4	3.7	65	15	18	2	0
	10	12	13	38	33	11	5

<sup>a</sup> Temperature of reaction (°C). <sup>b</sup> Time of reaction (h). <sup>c</sup> Conversion of cyclohexane (Cha). <sup>d</sup> Selectivities of cyclohexanol (Chol), cyclohexanone (Chone), adipic acid (AA), glutaric acid (GA), and succinic acid (SA).

### 2.1.5. Selective Oxidation of H<sub>2</sub>S via Chemical Looping

The selective oxidation of H<sub>2</sub>S to elemental S is a very attractive alternative to the Claus process but suffers several drawbacks. The selectivity can be affected by catalysts' efficiency and operating conditions, and catalysts usually suffer from deactivation. Another aspect to consider is that usually reactions must be performed at a low H<sub>2</sub>S concentration (typically a few % at most). Indeed, due to safety issues, a high concentration of H<sub>2</sub>S (mixed to oxygen) cannot be processed. Furthermore, the presence of oxygen does not allow the treatment of H<sub>2</sub>S in the presence of other combustible compounds, meaning that natural gas or biogas containing H<sub>2</sub>S cannot be treated directly. To overcome these drawbacks, in 2016, UCCS proposed an innovative approach for the selective oxidation of H<sub>2</sub>S to S using the "chemical looping" (CL) concept. Such processes involve an oxygen carrier which is reduced in the presence of a reductant and produces the desired product. Subsequently, the exposure of the reduced solid to an oxidant allows the re-oxidation and regeneration of the carrier. This is intrinsically a transient process which involves the use of circulating fluidized bed systems [38] or fixed-bed switching reactors. At the laboratory scale, the fixed-bed reactor, which is fed alternatively with the gas reactants, is usually the most appropriate, while circulating bed reactor systems are better adapted for industrial applications, and are already used in fluid catalytic cracking [39]. CL processes were initially proposed for total combustion but have since been studied for several reactions of industrial interest, such as the reforming reaction [40,41]. When applied for the selective

oxidation of  $\text{H}_2\text{S}$  to elemental sulfur, the concept of CL consists of separating the reaction into two distinct steps (1 and 2):



where OCox and OCred represent the oxygen carrier in the oxidized and reduced forms, respectively.

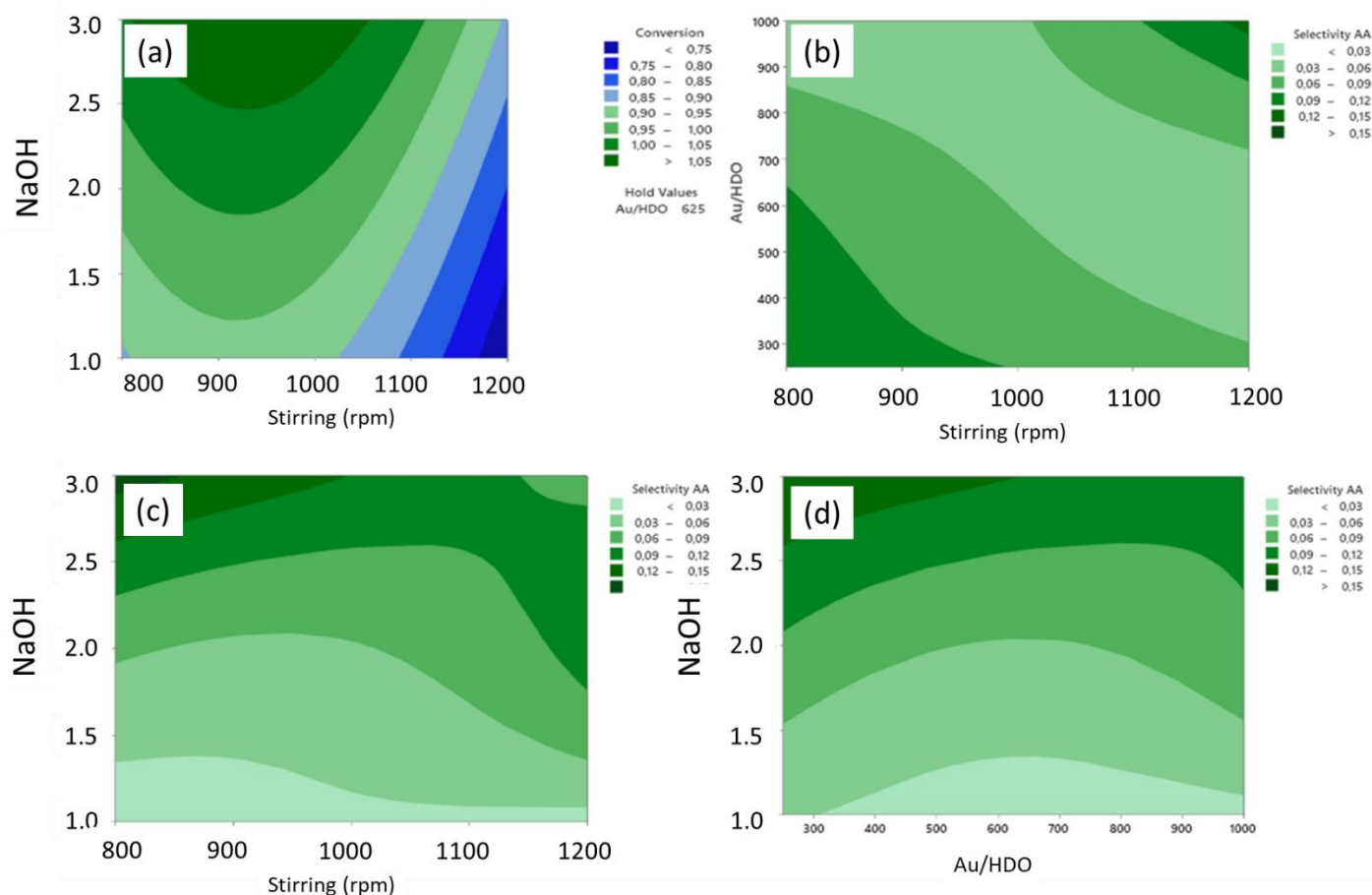


**Figure 6.** Contour plots of HDO conversion (a) and adipic acid selectivity versus (b) Au/HDO ratio and agitation, (c) NaOH equivalent and agitation, (d) NaOH equivalent and Au/HDO ratio.

The advantages of CL with respect to direct, co-feed, and oxidation reactions are the following: selectivity can be improved by avoiding a direct interaction between adsorbed sulfur species and di-oxygen from the gas phase or adsorbed onto the surface of the material and favoring the reactivity of lattice oxygen species; sulfur species deposited on the surface of the carrier can be removed during the regeneration step, thus avoiding the deactivation of the process; no mixing of  $\text{H}_2\text{S}$  and  $\text{O}_2$  can improve the safety of the process and enlarge the range of  $\text{H}_2\text{S}$  concentrations which may be processed; the preferential oxidation of  $\text{H}_2\text{S}$  could be performed in the presence of other combustible gases such as methane.

In the last case, if the preferential oxidation of  $\text{H}_2\text{S}$  is achieved in the presence of methane, then the direct purification of natural or biogas could be performed without the need of prior separation of  $\text{H}_2\text{S}$ , presenting a major breakthrough in natural and biogas treatments.

The idea of applying chemical looping to the selective oxidation of  $\text{H}_2\text{S}$  was proposed in 2016 through a patent application [42]. Since then, fundamental research has been performed on the topic and the validity of this concept has also been tested in industrial

process conditions and in the presence of impurities. The key to such a development is in the oxygen carrier, which needs to fulfill specific requirements. It should have:

- A high reactivity in both the oxidation and the regeneration reactions;
- A good selectivity for the desired oxidation product, i.e., elemental sulfur;
- A good stability over many redox cycles;
- A good resistance towards sulfur deposition and removal.

Other properties such as a good mechanical resistance in circulating bed systems will be required for the industrial implementation of the process.  $V_2O_5$  is well known for its oxygen mobility and storage capacity and catalytic reactivity for  $H_2S$  oxidation [43]. It was therefore chosen as a potential oxygen carrier in the chemical looping mode after checking the thermodynamic feasibility of the process on this material.  $V_2O_5$  proved to be highly reactive and selective towards elemental sulfur at rather low temperatures (150–200 °C) [44]. It could be seen that even at such low temperatures, sub-surface V species are involved in the looping process and not only surface species. On the contrary, it is suspected that uppermost surface species would be responsible for unselective  $SO_2$  production in the reductant step (i.e., during exposure to  $H_2S$ ). Depending on the reaction conditions, some deactivation of the system could be observed, but characterizations performed on used samples suggest that sulfur accumulation should not be responsible for this. The typical oxide materials used for supporting catalysts, such as  $TiO_2$ ,  $SiO_2$ ,  $CeO_2$ ,  $Al_2O_3$  or  $ZrO_2$ , have been considered for supporting the  $V_2O_5$  active phase [45]. Some of these materials show their own redox capacity, which may interfere with the looping process, as in the case of  $CeO_2$ . Otherwise,  $TiO_2$  and  $SiO_2$  have been identified as the most promising supports as they provide analogous or even better performances in comparison with bulk  $V_2O_5$ .

A deeper investigation into  $V_2O_5$  supported on  $TiO_2$  [46] has shown that optimal performances could be reached for the carrier containing the equivalent of two monolayers of  $V_2O_5$  dispersed on the surface of the support. Lower loadings tend to generate very reactive but less selective active species. Furthermore, as the absolute oxygen capacity of the carrier is dependent on the amount of  $V_2O_5$ , low-loading carriers rapidly reach the limit of  $H_2S$  transformation. This induces adsorbed  $H_2S$  to be converted to  $SO_2$  in the regeneration step. Furthermore, it may also lead to the over-reduction of the vanadium species, which are suspected to be less selective towards elemental S. For higher loading, the formation of tower-like  $V_2O_5$  structures on the surface of the support seems to be detrimental to the reactivity of the carrier. Several phenomena may occur. First, larger crystallites exhibit a higher proportion of  $V^{5+}$  species (with respect to  $V^{4+}$ ), which are less reactive or less selective, in particular for surface species with respect to bulk ones. Second, in the case of tower-like structures, bare  $TiO_2$  can still be exposed, even at high loadings. This can lead to  $H_2S$  adsorption generating higher amounts of  $SO_2$  produced during the oxidant (regeneration) step. Finally, the textural properties of the support have been proved to be very important for this process with respect to the selectivity towards elemental sulfur. A support with higher porosity may induce consecutive reactions in the reductant step and thus the over-oxidation of product, but also the accumulation of adsorbed sulfur species (e.g., elemental S produced, or unreacted  $H_2S$ ). These would then be oxidized in  $SO_2$  during the regeneration steps, contributing to low selectivity. The study performed on the optimal loading of  $V_2O_5$  (two monolayers) onto  $TiO_2$  with a low surface area further confirms the importance of finding a good balance between vanadium species in different valence states. All results suggest that the best selectivity in elemental sulfur is obtained when  $V^{5+}$  to  $V^{4+}$  reduction occurs, whereas  $V^{4+}$  to  $V^{3+}$  reduction seems to be more favorable for unselective oxidation. On the other hand, highly oxidized systems with high proportions of  $V^{5+}$  seem to be less reactive and slightly less selective, as already mentioned. The optimal situation is when approx. 30% of V is converted from  $V^{5+}$  to  $V^{4+}$ , but starting from materials which already contain significant proportions of  $V^{4+}$  (>30%).

## 2.2. Reactions Involving Hydrogen

### 2.2.1. Carbohydrate Hydrogenation

The hydrogenation of the carbonyl groups of carbohydrates leads to the formation of polyols. Industrially, the three most important polyols are: sorbitol (from glucose) [47,48], xylitol (from xylose) [49] and maltitol (from maltose) [50]. In the case of xylitol, for example, the global industrial production is estimated to be about around 200 kt/year. The hydrogenation of xylose is usually performed in aqueous solutions using batch reactors at temperatures between 100 and 150 °C under high pressures of H<sub>2</sub> (up to 50 bar). Comparable conditions are also applied in the case of glucose and maltose hydrogenations. Generally, these hydrogen-related processes are carried out on noble metals such as Ru, Pd, Pt and Ru, but Raney Ni is also used, especially in industrial applications. The VAALBIO group is working on different aspects of these processes: developing new catalysts, improving the stability of the existing catalysts and studying the kinetic aspects of the reaction. Recently, we studied new Ni-Fe-based catalysts for maltose and xylose hydrogenation in water. The Ni-Fe alloy is a good option to replace nickel catalysts. A Ni<sub>62</sub>Fe<sub>38</sub>/SiO<sub>2</sub> bimetallic catalyst prepared by deposition–precipitation with urea (DPU) showed high activity in the hydrogenation of xylose and maltose in water [49,50]. We showed that the temperatures of 50–80 °C are most favored due to the limitation of the metal leaching and the presence of a kinetic regime even for high masses of the catalyst. The Ni<sub>62</sub>-Fe<sub>38</sub>/SiO<sub>2</sub> catalyst exhibits a higher catalytic activity than the monometallic Ni catalyst. The selectivity to xylitol and maltitol (in the case of maltose hydrogenation) remained optimal and constant (~100%), even after three consecutive runs. The stability of the bimetallic catalysts was also better as compared to the Ni<sub>100</sub>/SiO<sub>2</sub> catalyst (Figure 7), which showed a decrease in the catalytic activity after the first catalytic test, which is associated with a more pronounced formation of the initial Ni<sup>2+</sup>-phyllosilicate phase [49].

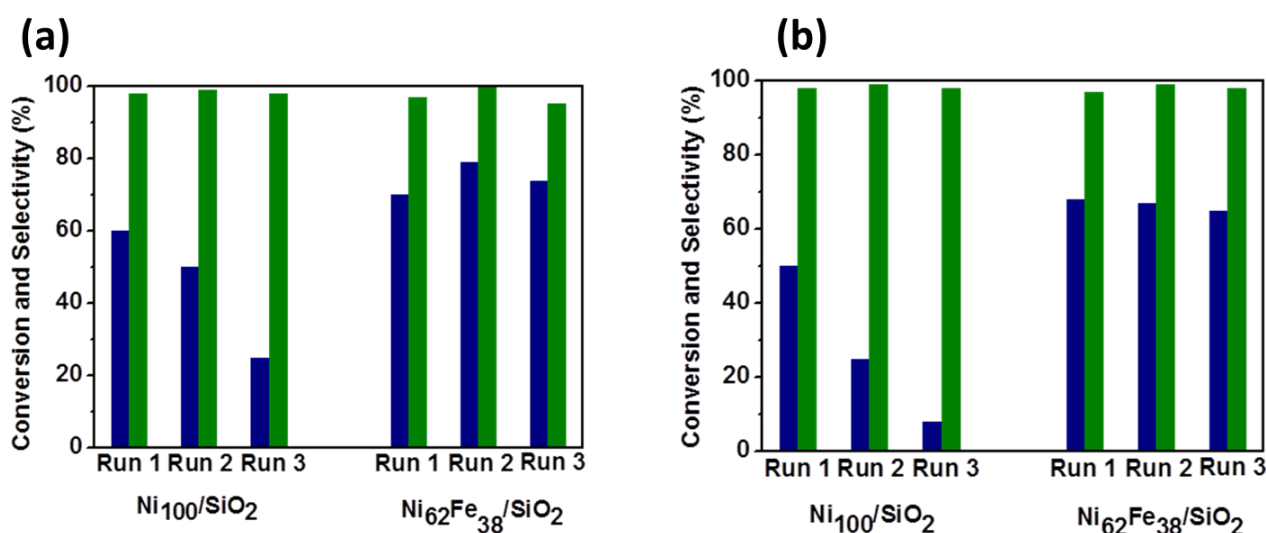


**Figure 7.** Catalyst recyclability study: (a) blue bars represent xylose conversion; green bars represent xylitol selectivity. Reaction conditions: Xylose—0.26 mol L<sup>-1</sup>; 20 bar H<sub>2</sub>; 80 °C; 108 mg catalyst; 90 min reaction time;  $n_{\text{xylose}}/n_{\text{Ni}} = 9.7$ ;  $n_{\text{xylose}}/n_{\text{Ni}} + n_{\text{Fe}} = 10.6$ . (b) Blue bars represent maltose conversion; green bars represent maltitol selectivity. Reaction conditions: 8.8 wt.% maltose; 20 bar H<sub>2</sub>; 80 °C; 108 mg catalyst; reaction time = 8 h;  $n_{\text{maltose}}/n_{\text{Ni}} = 9.8$ ;  $n_{\text{maltose}}/n_{\text{Ni}} + n_{\text{Fe}} = 10.0$ . Adapted with permission from Refs. [49,50].

In the case of the glucose hydrogenation, we applied the high-throughput (HT) methodology for each step of the process: synthesis, characterization and catalytic testing. In total, 36 Ni and Cu catalysts were prepared by chemical reduction with the hydrazine method [48]. We chose the amount of Ni or Cu deposited on the support as the discriminative parameter. The results showed that the deposition of nickel and copper on the

oxide strongly depended on the nature of the support ( $\text{SiO}_2$  or  $\text{Al}_2\text{O}_3$ ), the hydrazine/ $\text{H}_2\text{O}$  ratio and the temperature of the reduction. The optimal conditions were as follows: high temperature ( $70^\circ\text{C}$ ) and low  $\text{N}_2\text{H}_4/\text{H}_2\text{O}$  ratio (0.04 mol/mol), irrespective of the metal precursors. The best catalytic results were obtained for the 5%Ni deposited on  $\text{Al}_2\text{O}_3$  and 5% Cu deposited on  $\text{SiO}_2$  (Figure 8), synthesized at  $70^\circ\text{C}$ .

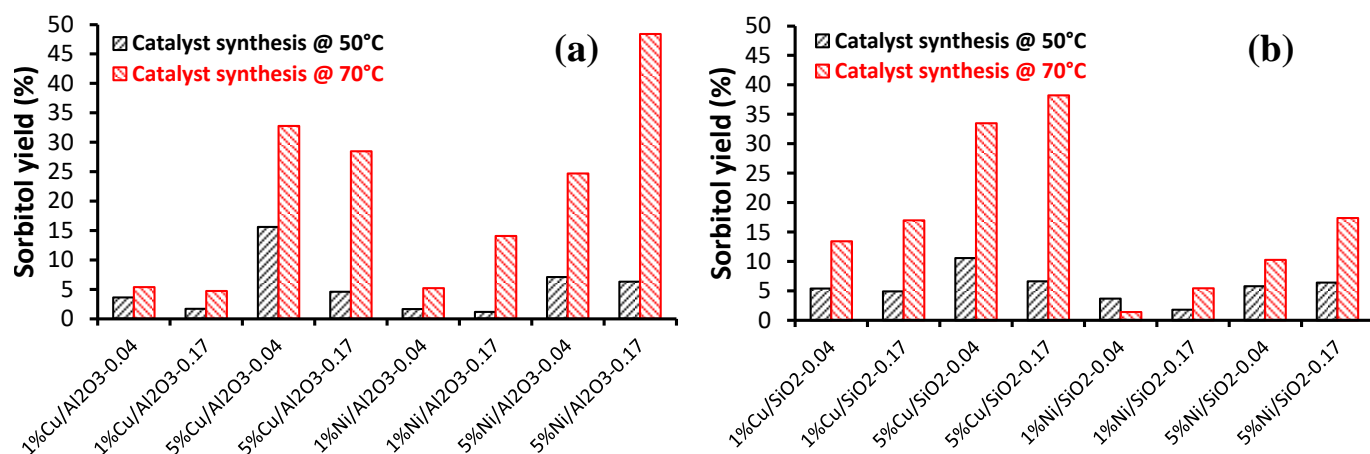


**Figure 8.** Sorbitol yields with (a) alumina-supported and (b) silica-supported catalysts synthesized at temperatures of 50 and  $70^\circ\text{C}$ . (Test conditions: catalyst amount = 10 mg; 3 mL of glucose solution (1 wt.%);  $T = 130^\circ\text{C}$ ;  $P_{\text{H}_2} = 30$  bar;  $t = 4$  h). Adapted with permission from Ref. [48].

### 2.2.2. Furanics Hydrogenation

Quite a large number of metals can effectively catalyze furfural and HMF hydrogenation: Pt, Pd, Ru, Au, Rh, Ni, Cu, Co, and Fe [23,51–53]. A variety of products can be obtained. The selectivity of the transformation becomes, in this case, a key parameter. In most cases, the excessive hydrogenation of the furan ring and hydrogenolysis, which may involve (a) the alcohol group, (b) the opening of the heterocycle, and (c) the C–C bond of the ring-aldehyde, should be avoided [23,51]. When the transformation requires consecutive steps, the order in the hydrogenation/hydrogenolysis sequence must be carefully controlled. Thus, the key to realizing selective transformations is the proper tuning of the reaction system, both in terms of catalytic and experimental conditions. Most of the catalysts investigated in recent decades for the reductive conversion of FF and HMF are noble metal-based catalysts [54–56]. Noble metals show high hydrogenation activity, but their resources are limited. Base metals, such as iron, nickel and copper, are more available and less expensive. These systems can be optimized by combining them with other metals and by selecting the appropriate carrier, solvents, and/or co-catalysts (e.g., mineral acids).

Iron (Fe) and nickel (Ni) are two non-precious metals that can be used for the hydrogenation of organic molecules. While monometallic Ni is known to promote undesirable side reactions of hydrogenation and ring opening, Fe–Ni bimetallic catalysts have shown interesting properties for the selective hydrogenation of alcohol and aldehyde groups [57]. Fe–Ni/ $\text{SiO}_2$  catalysts were tested in the liquid-phase furfural hydrogenation reaction at  $150^\circ\text{C}$  under 20 bar  $\text{H}_2$  [58,59]. The conversion of furfural increased rapidly with an increasing Ni content. The highest yield of furfuryl alcohol was obtained with Fe–Ni catalysts containing 60–75% at. Ni. An increasing Ni content systematically increases the consumption of furfuryl alcohol (FFA) through three parallel secondary reactions: etherification with isopropanol solvent, possibly catalyzed by metal ions that remain unreduced after activation. The formation rates of isopropyl furfuryl ether (iPrOMF), methylfurfural (MF), and tetrahydrofurfuryl alcohol (THFFA) from FFA also increased with Ni content. For catalysts with Ni content in the active phase lower than 84 wt.%, FFA is mainly consumed in the hydrogenolysis reaction to MF, in the slower etherification reaction to iPrOMF, and in the furan ring hydrogenation reaction to THFFA. For catalysts with a Ni content in the active phase higher than 84 wt.%, FFA is consumed mainly by etherification to iPrOMF, by

the slower second hydrogenolysis route to MF and by the even slower hydrogenation of the furan ring to THFFA [59].

Nickel catalysts were also studied in HMF hydrogenation. We showed that a monometallic Ni/SBA-15 catalyst, prepared by incipient wetness impregnation, is able to convert HMF to 2,5-dimethylfuran (DMF) and 2,5-dimethyltetrahydrofuran (DMTHF) at 180 °C. This process occurs in two consecutive steps [60]. By controlling the reaction time, high yields to DMF (71%) or DMTHF (97%) at high conversion (97–100%) can be obtained (Figure 9).

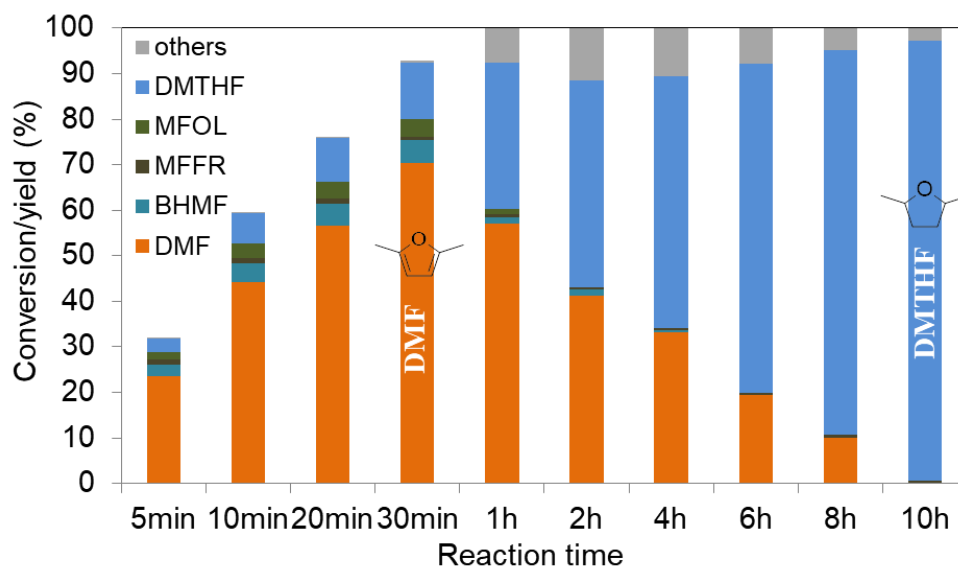


**Figure 9.** Evolution of HMF conversion and product yields with reaction time over Ni/SBA-15. Reaction conditions: 0.144 mmol/mL HMF in 25 mL 1,4-dioxane;  $P(H_2) = 30$  bar;  $T = 180$  °C; HMF/Ni molar ratio of 3. Reprinted with permission from Ref. [60].

Kinetic studies suggest that 5-hydroxymethylfurfural is converted via MFFR as an intermediate. It was shown that the C-O hydrogenolysis and C=O hydrogenation routes are much faster than the furan ring hydrogenation.

### 2.2.3. Allyl Alcohol Synthesis from Glycerol

The use of sustainable resources for the synthesis of olefinic compounds is of much interest due to the importance of the latter as platform chemicals. As example, allyl alcohol is a promising platform molecule due to its broad range of applications. Its derivatives are present in resins, pharmaceutical products, perfumes and food formulations. Furthermore, allyl alcohol is considered as a promising starting material of important intermediates for the chemical industry, such as acrylonitrile and acrylic acid, which have large-scale applications for polymers and resins. Hereby, UCCS has developed catalysts for the whole value chain, starting from glycerol to acrylic acid and acrylonitrile via allyl alcohol as an intermediate (Figure 10).

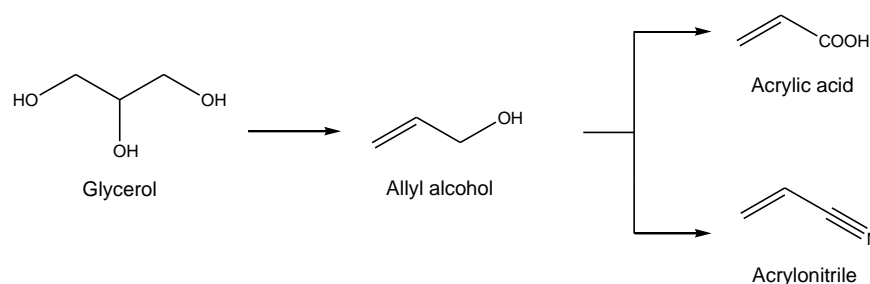


**Figure 10.** Production of important intermediates of the chemical industry using allyl alcohol from glycerol as an intermediate.

In fact, among the various bio-based pathways to allyl alcohol, those starting from glycerol are particularly interesting since it is the main by-product of the biodiesel industry. Glycerol is considered as a potential biorefinery feedstock to develop various processes of valuable chemicals such as glyceric acid, acrolein, 1,2-propanediol and polyglycerol [61–64]. With the growing demand for sustainability, there has been increased attention on glycerol conversion toward less oxygenated derivatives, making it a preferred starting material for the synthesis of allyl alcohol. The transformation of glycerol to allyl alcohol has been focused on selective oxygen removal via the deoxydehydration reaction (DODH), a very competitive methodology which has been poorly investigated. The DODH reaction consists of the removal of two vicinal hydroxyl groups from a diol or polyol to yield the corresponding alkene (C=C bond). Figure 11 displays the case of the DODH of glycerol to allyl alcohol [65]. This reaction requires a stoichiometric reductant (red), which is oxidized during the reaction (redO).

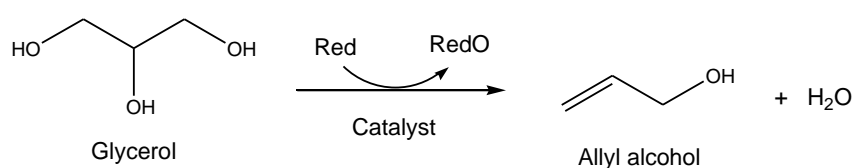


**Figure 11.** General reaction pathway for the deoxydehydration reaction. Red = reductant. RedO = oxidized reductant [66].

An array of catalytic processes of the DODH of glycerol have been reported in the literature, including homogeneous [67] and heterogeneous catalysis [66,68,69]. The identification of an optimal reductant/catalyst couple has been a focus of research at UCCS. A catalyst for the DODH of glycerol to allyl alcohol using 2-hexanol as hydrogen was developed based on alumina-supported rhenium oxide [66]. The main drawback of this catalytic system is the co-produced ketone, namely, 2-hexanone. This molecule has a high toxicity and no profitable value can be envisaged. Consequently, the alcohol has to be regenerated in order to avoid ketone accumulation. Thus, a ceria-supported rhenium oxide catalyst was developed in combination with an alternative secondary alcohol—methyl isobutyl carbinol (MIBC). The employed mesoporous ceria support was synthesized via a nanocasting process using  $\text{SiO}_2$  and activated carbon as hard templates and impregnated with  $\text{ReOx}$  [70]. The resulting catalysts give excellent yields of up to 86%, with MIBC as a hydrogen donor and solvent, forming not only allyl alcohol as a valuable product, but also a stoichiometric amount of methyl isobutyl ketone (MIBK), a valuable organic solvent used in liquid–liquid extraction.

### 2.3. Reactions under Specific Atmosphere ( $\text{CO}_2$ , $\text{NH}_3$ and $\text{N}_2$ )

#### 2.3.1. Direct Carboxylation

$\text{CO}_2$  is also a valuable substrate for the synthesis of high-added-value molecules. The direct catalytic and sustainable carboxylation of aromatic molecules using a “simple” insertion of carbon dioxide into the  $\text{sp}^2$  C-H bond is highly desirable. In 1860, Kolbe reported the direct carboxylation of phenol with  $\text{CO}_2$  (Kolbe–Schmitt synthesis) [71]. Kolbe and Schmitt showed that the phenol group plays a crucial role in this reaction. Since then, various carboxylation processes have been studied. The most important are: (i) the Henkel reaction, (ii) enzymatic reactions, (iii) molten salts, (iv) homogeneous catalysis and (v) photo-electrocatalytic processes. However, many challenges are faced in these processes [35]. 2,5-Furandicarboxylic acid (FDCA) is a very important building block for the synthesis of polymers such as poly(ethylene furandicarboxylate) (PEF). PEF is generally proposed as an alternative to poly(ethylene terephthalate) (PET), a non-sustainable monomer [72]. The possibility of FDCA production from hemicellulose is of high interest from an industrial point of view. Furfural, which is already implemented in industrial production from non-edible resources, could act as a substitute for HMF. As illustrated in Figure 12, the catalytic oxidation of furfural forms 2-furoic acid. It can then undergo the direct C-H

carboxylation with CO<sub>2</sub> to produce FDCA [72,73]. These two catalytic processes can be performed sequentially (Figure 12) [72,73].

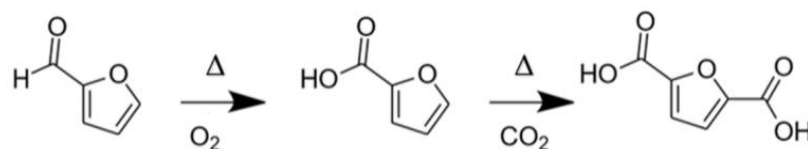


**Figure 12.** Two-step FDCA synthesis method of furfural using oxidation and carboxylation steps.

However, the main challenge of this process is inserting the carboxylate group into the C-H bonds [72]. CO<sub>2</sub> is a C1 feedstock and presents kinetic and thermodynamic limitations [35,73]. Recently, we proposed a proof-of-concept process using heterogeneous catalysts for the direct carboxylation of furoic acid using Henkel reaction conditions (devices, temperature, and catalyst/reactant ratio). The use of the Henkel reaction to selectively produce FDCA from furoic acid salt (K<sub>2</sub>F) using CdI<sub>2</sub> as a catalyst has already been reported [72]. However, the minimum reaction temperature is 260 °C. At this, CdI<sub>2</sub> starts to decompose, which improves the interaction between the semi-melted catalyst and the solid K<sub>2</sub>F. In order to reduce the working temperature, a heterogeneous catalyst was applied in addition to the CdI<sub>2</sub> co-catalyst (Table 3).

**Table 3.** Effect of the temperature on FDCA synthesis from K<sub>2</sub>F using Ag/SiO<sub>2</sub> and CdI<sub>2</sub> catalysts. Conditions: 17 mg of CdI<sub>2</sub>; 35 mg of K<sub>2</sub>F; 50 mg of Ag/SiO<sub>2</sub>; F<sub>N<sub>2</sub></sub> = 45 mL/min; 20 rpm; T = 200–260 °C; t = 20 h. Adapted with permission from Ref. [72].

Catalyst	Temperature (°C)	Conversion (%)	STY <sub>FDCA</sub> (μmol kg <sup>-1</sup> h <sup>-1</sup> )	STY <sub>DFP</sub> (μmol kg <sup>-1</sup> h <sup>-1</sup> )
CdI <sub>2</sub>	200	0	-	-
Ag/SiO <sub>2</sub> + CdI <sub>2</sub>	200	51	264	951
Ag/SiO <sub>2</sub> + CdI <sub>2</sub>	230	74	145	-
Ag/SiO <sub>2</sub> + CdI <sub>2</sub>	260	69	188	-
Ag/SiO <sub>2</sub>	200	20	1203	-

Using a dual catalytic system, the reaction temperature was decreased to 230 °C since the K<sub>2</sub>F conversion did not change. The FDCA yield was not significantly affected when using both catalysts. When a 2 M HCl solution was applied to extract the crude product from the reaction medium, a higher STY yield was obtained. In addition, using the heterogeneous Ag/SiO<sub>2</sub> catalyst permitted us to decrease the temperature to 200 °C [72].

### 2.3.2. Ammoxidation

The ammoxidation of allyl alcohol to acrylonitrile is the subject of only very few studies, notably due to the importance of acrylonitrile as an intermediate (USD 11.8 billion in 2019). In 2013, our team reported the use of antimony-iron catalysts of different Fe/Sb ratios (0.6 and 1) for the ammoxidation of acrolein with 36% yield [74]. The application of the same catalyst was then studied in the ammoxidation of allyl alcohol, yielding up to 86% acrylonitrile under optimized reaction conditions (0.16 s contact time, 450 °C, AllylOH/O<sub>2</sub>/NH<sub>3</sub> ratio 1/3.5/3) [75]. Surprisingly, both catalysts showed very similar performances despite the different Fe/Sb ratios. A detailed study of the surface composition by X-ray photoelectron spectroscopy (XPS) and low-energy ion scattering (LEIS) revealed that the surface layer of the catalyst was enriched in antimony after testing. The latter was ascribed to the formation of a FeSbO<sub>4</sub> mixed phase under reaction—which was also evidenced by an induction period of the catalytic test with the increasing formation of acrylonitrile during the first hours on stream.

### 2.3.3. Glycerol Polymerization

Glycerol polymers are highly demanded by industry. Different types of glycerol polymers can be obtained and thus directed to various target applications. Solid bases used as catalysts give the best performances, and, among them, the Ca-based catalysts are particularly considered as efficient [63]. Based on the analysis of spent calcium oxide and calcium hydroxide solids (X-ray powder diffraction and  $^{13}\text{C}$  solid-state NMR), we evidenced that the active phase is actually not the initial solid added to the medium, but rather a Ca-glycerolate phase (linear  $\text{Ca}(\text{C}_3\text{H}_7\text{O}_3)$  or cyclic-branched  $\text{Ca}(\text{C}_3\text{H}_6\text{O}_3)$ ) formed in situ [76]. We explained the formation of Ca-glycerolate, e.g., from CaO through a dissolution and precipitation followed by crystallization.

### 2.3.4. Butadiene Synthesis from Ethanol

1,3-Butadiene (1,3-BD) is a chemical intermediate of high interest in industry (USD 44.8 billion foreseen market value in 2026), especially due to its major application as a monomer for manufacturing synthetic rubber. However, the 1,3-BD supply and sustainability are at stake and alternative production routes are desired to at least partly get rid of the steam cracking of naphtha dependency. Realizing 1,3-BD production from bioethanol would fully unlock the value chain and enable a sustainable supply while, if correctly handled, yielding a lower environmental impact [77,78]. By combining screening methods to design experiment to optimize the catalytic formulations, [79] we rationalized the design of highly productive catalysts. Lab-made Zn-Ta-TUD-1, with Zn:Ta (mol:mol) between 1.5 and 2 and presenting a high specific value of  $>600 \text{ m}^2 \cdot \text{g}^{-1}$  with an average pore diameter of around 10 nm, was found to be very efficient [80]. With such a catalytic formulation, it was possible to realize the remarkable 1,3-BD productivity of  $2.45 \text{ g } 1,3\text{-BD g}_{\text{cat}} \text{ h}^{-1}$  with performances over 60 h being much more stable than those of conventional catalysts. We found that the active phase is made up of highly dispersed Zn(II) species together with tetrahedral isolated species and monolayered clusters of Ta(V) (FTIR, UV-Vis-DRS, XPS, XRD and HR-STEM) [81].

### 2.4. $\text{H}_2$ Production from Bioresources (Biomass and Biogas)

Hydrogen is an important chemical product, as the most used gas in the industry and also for the future “green” energy, that can be used directly by combustion or in combination with a fuel cell, leading to electricity. Today,  $\text{H}_2$  is mainly produced from fossil resources; it is urgent to produce it from renewable resources, not only so it can really be “green” but also to follow its increasing demand. Even if some  $\text{H}_2$  sources have been recently found, hydrogen is mainly found in numerous molecules (such as the simplest one, water, hydrocarbons, alcohols, etc.), so  $\text{H}_2$  needs to be produced. Therefore, at the international level, hydrogen production is largely studied, with the objective to use renewable resources and/or renewable energies. In this context,  $\text{H}_2$  production from ethanol (easily obtained from biomass) and from  $\text{CH}_4$  (biogas) are the subject of much research. To perform these reactions, noble metals (Pd, Pt, and Rh) and transition metals (Ni, Co, and Fe) with different bulk and supported catalysts have been extensively studied. Research has revealed that the redox properties and the strong metal–support interactions are the two key parameters to avoid sintering and carbon formation. Our objective was the development of ex-hydrotalcite (HT) compounds to enable us to incorporate metal cations for the selective production of hydrogen. Transition metal catalysts were preferred compared to the much more expensive noble metals ones, where Ni catalysts showed the best performances [82].

In the laboratory,  $\text{H}_2$  production is studied from ethanol by steam reforming (SRE), partial oxidation and oxidative steam reforming (OSRE, including autothermal reforming) reactions [82–86], and from  $\text{CH}_4$ , by dry reforming (DRM) and oxidative dry reforming (ODRM) reactions [40,87–90]. These last reactions are of particular interest because they allow the transformation and valorization of two greenhouse gases ( $\text{CH}_4$  and  $\text{CO}_2$ ), and also can be applied to fuel cells [90]. Different types of Ni-based catalysts such as  $\text{CeNi}_x\text{Al}_{0.5}\text{H}_z\text{O}_y$

( $0 < x \leq 5$ ,  $z = 0$  or  $0.5$ ) [40,82,83,87–89] and  $\text{Ni}_x\text{Mg}_2\text{AlO}_y$  ( $0 < x \leq 12$ ) [82–84] compounds were developed, with the objective to obtain highly performant, selective and stable catalysts. Ni-based catalysts are particularly interesting due to their ability to promote C–C-bond cleavage, participation in the water gas shift reaction and high performance in methane reforming. The influence of different parameters was analyzed to optimize the catalytic material (preparation, formulation, Ni content, and pretreatment) and the operational conditions (reactant concentration, reaction temperature, presence of  $\text{O}_2$  in the feed, etc.), including the chemical looping reaction [40,87–89].

Optimizing the proportion of Ni cations ( $\text{Ni}^{2+}$ ) in strong interactions with other cations and the presence of anionic vacancies in the mixed oxides allow the formation of oxyhydride compounds, leading to particularly interesting material properties and mechanisms, involving the heterolytic abstraction of hydride species from ethanol (Figure 13a) [83] and from  $\text{CH}_4$  (Figure 13b) [89].

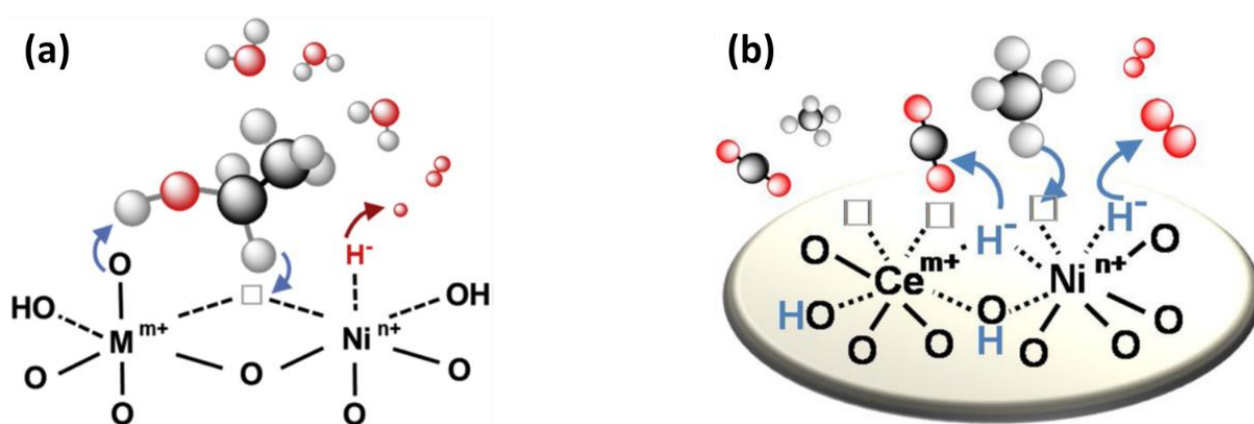


**Figure 13.** (a) OSRE on  $\text{Mg}_2\text{AlNi}_x\text{H}_z\text{O}_y$  oxyhydride catalysts.  $\text{Ni}^{n+}$ :  $\text{Ni}^{2+}$  or  $\text{Ni}^{\delta+}$ ,  $\text{M}^{m+}$ :  $\text{Mg}^{2+}$  or  $\text{Al}^{3+}$  and  $\square$ : anionic vacancy. The positions of anionic vacancy and hydride species are arbitrary [85]; (b) ODRM on  $\text{CeNi}_x\text{Al}_{0.5}\text{H}_z\text{O}_y$  oxyhydride catalysts.  $\text{Ni}^{n+}$ :  $\text{Ni}^{2+}$ ,  $\text{Ni}^{\delta+}$ ,  $\text{Ce}^{m+} = \text{Ce}^{4+}$ , and  $\text{Ce}^{3+}$  ( $\text{Al}^{3+}$  can replace a cerium cation in the solid solution).  $\square$ : anionic vacancy, red balls: oxygen, black balls: carbon, white balls: hydrogen. The positions of anionic vacancy and hydride species are arbitrary [89].

For example, using these properties, we developed particularly efficient cerium and Ni-based catalysts for ethanol transformation at room temperature, as well as a new technology, in the presence of oxygen in the feed [82].  $\text{Mg}_2\text{AlNi}_x\text{H}_z\text{O}_y$  nano-oxyhydrides were also shown to be highly performant in SRE and OSRE with high stability [86]. Carbon formation is decreased and a much lower input of energy of  $50^\circ\text{C}$  is used to reach a temperature of  $300^\circ\text{C}$  when  $\text{O}_2$  is added. Moreover, a higher production of  $\text{H}_2$  can be achieved at a reaction temperature of  $300^\circ\text{C}$  in OSRE conditions compared to SRE ( $60$  instead of  $10\text{ L h}^{-1}\text{ g}_{\text{cat}}^{-1}$ ), mainly because of the beneficial use of a high concentration of ethanol ( $14\text{ mol. \%}$ ) in the presence of  $\text{O}_2$ . For  $\text{H}_2$  production from methane,  $\text{CeNi}_x\text{Al}_{0.5}\text{H}_z\text{O}_y$  ( $0.5 \leq x \leq 5$ ) nano-oxyhydride catalysts were shown to be highly performant in ODRM ( $\text{CH}_4/\text{CO}_2/\text{O}_2/\text{N}_2 = 1:0.7:\alpha:\text{N}_2$  with  $20\%$  of  $\text{CH}_4$  and  $\alpha$  varying from  $0$  up to  $0.5$ ,  $96,000\text{ mL h}^{-1}\text{ g}_{\text{cat}}^{-1}$ ) [89]. At  $500^\circ\text{C}$ , the  $\text{CO}_2$  conversion overcomes the predicted value and the conversion of  $\text{CH}_4$  reaches the thermodynamic limit. At  $600^\circ\text{C}$ , with an  $\text{O}_2/\text{CH}_4$  ratio of  $0.3$ , the  $\text{CeNi}_x\text{Al}_{0.5}\text{H}_z\text{O}_y$  catalyst allows  $\text{CH}_4$  and  $\text{CO}_2$  conversions of about  $63\%$  and  $50\%$ , respectively, and a  $\text{H}_2/\text{CO}$  ratio of about  $1.3$ , without carbon formation.

### 2.5. Biomass Fractionation

Lignocellulosic biomass is an abundant, non-edible and renewable resource for the production of high value-added chemicals and fuels in future biorefineries. However, the use of this sustainable raw material as a feedstock requires the development of new chemical processes and catalysts. The conversion of lignocellulosic biomass into chemicals

and fuels in a biorefinery involves a multi-step process: the fractionation of lignocellulosic biomass into its main components (cellulose, hemicellulose and lignin), followed by depolymerization and upgrading. These steps are performed separately or consecutively, which increases the costs. In addition, lignin is most often considered to be a waste and is burned for energy generation in first-generation biorefineries. These goals can be achieved with novel fractionation technologies that operates at low temperatures, which opens up the possibility for the integration of chemical and biological catalysis and the use of hybrid catalysts, in which chemical and biological catalysts work in tandem in one-pot and one-step reactions. However, these alternative processes require the design of more efficient and selective catalysts. Recently, a two-step processing of lignocellulosic biomass was previously carried out using acidic molten salt hydrate [91]. Inorganic molten salt hydrates are concentrated inorganic salt solutions with a water to salt molar ratio close to the coordination number of the strongest hydrated cation, with the water molecules bound to the inner coordination sphere of the cation, while the anion is free in solution [92–94]. They are inexpensive, easy to prepare and environmentally friendly as no toxic and volatile organic compounds are required to prepare such solvents. Moreover, the inorganic salts can be recovered by evaporating the water after cellulose regeneration and can be recycled for further use [95].

Inorganic molten salt hydrates are known to dissolve cellulose, which depends on the water content as well as the structure of the cation coordination sphere [92,95–97]. The interaction between the cation and cellulose weakens and breaks the intra- and inter-molecular hydrogen bonds of the cellulose chains. Different inorganic molten salt hydrates have the ability to dissolve cellulose (Figure 14), such as: LiBr, LiCl, ZnBr<sub>2</sub>, ZnCl<sub>2</sub>, FeBr<sub>2</sub>, and FeCl<sub>3</sub> [92,97]. The dissolution of cellulose in inorganic molten salt hydrates decreases its crystallinity, which improves the reactivity of cellulose. Various inorganic molten salt hydrates have been used for cellulose hydrolysis under mild conditions (low acid concentration and temperature) [95,98,99]. The hydrolysis rate and product distribution are affected by the type and concentration of the inorganic molten salt hydrate, reaction temperature and the concentration of acid. Glucose, fructose, levoglucosan, HMF and levulinic acid are the major products reported, with the yield of each product depending on the type of molten salt hydrate. Once cellulose and hemicellulose are extracted from the biomass matrix, they are transformed into platform molecules by using a heterogeneous catalyst. Different commercial solid acid catalysts with various acidity values could be used (Amberlyst, Dowex, Nb<sub>2</sub>O<sub>5</sub>, NbPO<sub>4</sub>, ZrO<sub>2</sub>, SO<sub>3</sub>-ZrO<sub>2</sub>, ZSM-5, and USY). A catalyst containing highly active transition metal nanoparticles and acid sites deposited on an inorganic support was designed. The reaction involves the hydrolysis of the carbohydrates on the sulfonic groups grafted onto the silica support followed by the hydrogenation of the sugars produced on the metal (Ru and Pd) particles into sorbitol and xylitol, which are platform molecules. Lignin remains in the solid residue produced and it is separated and catalytically transformed into hydrocarbons by hydrodeoxygenation.

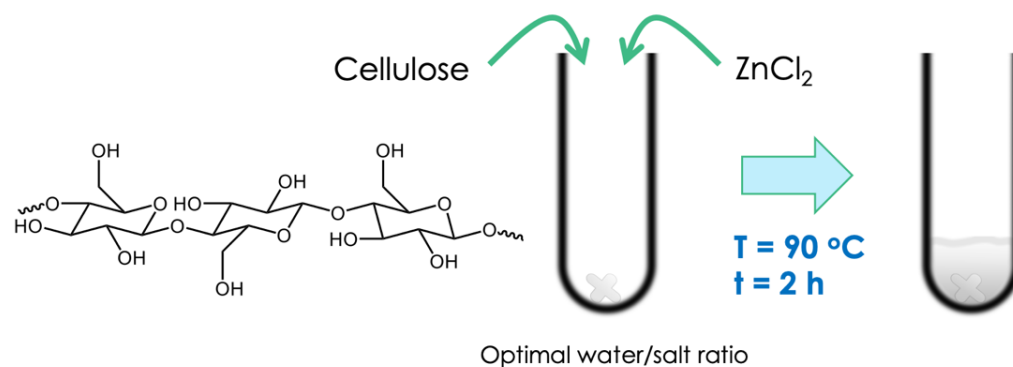


**Figure 14.** Example of cellulose hydrolysis using molten salt methodology.

## 2.6. Hybrid Catalysis

In recent years, industrial biotechnology has had a significant impact on the pharmaceutical and chemical industries, backed up by advances in the field of enzyme evolution aimed at building new enzymes and catalysts. This has led to the development of more efficient manufacturing processes, while producing less waste and avoiding the use of harmful solvents and reagents [100]. Consumer demands for green and sustainable products with minimal environmental impact have been one of the biggest drivers of finding more sustainable routes in order to obtain compounds of great industrial value. Within this frame, chemical catalysis and enzymatic catalysis have moved closer to one to another, towards the innovative interdisciplinary concept of hybrid catalysis that aims to couple these different “worlds” in the same reactor [101]. This enables the improvement of reactions’ performances and yields new synthesis pathways through the combination of the best characteristics of each system, which must be first optimized separately before merging [102–104]. Such an approach is still rather scarcely developed at the international scale, while considerable growth can be expected in the mid-term. In this context, we are involved in some pioneering works. While such a combination has been long considered as inconceivable, we have demonstrated its relevance through a few different variations of the concept among the scope of possibilities it opens [2,105]. Hereafter is an overview of the achieved results in the field of hybrid catalysis by the VAALBIO team.

### 2.6.1. Enhanced Dynamic Kinetic Resolution

Among the various strategies for separating two enantiomers in a racemic mixture, the kinetic resolution (KR) and the dynamic kinetic resolution (DKR) have been of great importance in global chemistry [106]. In a KR, enantiomers react with different reaction rates and selectivities in reaction with a catalyst, biocatalyst or chiral reagent, resulting in an enantio-enriched sample of the less reactive enantiomer. However, a crucial limitation of KR is that the maximum theoretical yield is 50%. One solution is the combination of a chemical catalyst capable of racemizing the unwanted enantiomer in situ. In this way, the racemate obtained returns to the KR process [107,108]. This process is named dynamic kinetic resolution (DKR) and a theoretical yield of 100% can be achieved. This strategy has been successfully applied to a wide range of other compounds, such as chiral amines. Generally, racemization requires thermal or strongly acidic or basic conditions that are incompatible with a stereo-transformation into a single batch reactor or in continuous processes. On the other hand, several transition metal complexes such as rhodium, ruthenium and iridium are known to catalyze the racemization of optically active amines under mild conditions [109]. One solution to this is the use of hybrid catalysts, which involves cooperation between an enzyme and metal catalyst [110]. Among the numerous enzymes that have been applied in DKR for obtaining enantiomerically pure amines, lipases (triacylglycerol hydrolases, *E.C.* 3.1.1.3) are the most widespread group [110]. A number of published procedures that take advantage of a reagent/chemical catalyst chemical to perform dynamic kinetic resolution have been reported (Figure 15).

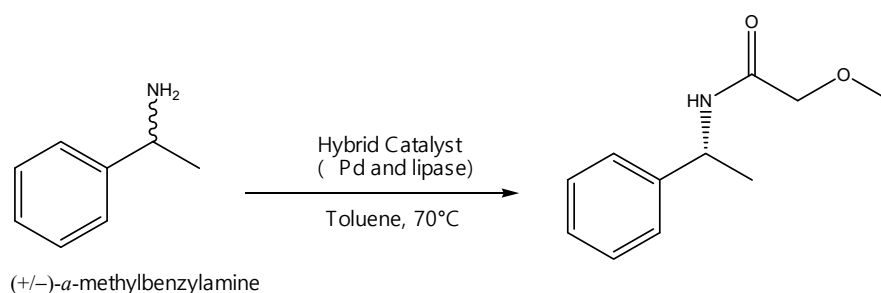


**Figure 15.** Example of DKR reaction using hybrid Pd-lipase system [111].

For example, supported Pd nanoparticles with immobilized lipases have been shown to facilitate this reaction, as shown below (Table 4) [111].

**Table 4.** Dynamic kinetic resolution of  $\alpha$ -methylbenzylamine catalyzed by hybrid catalyst.

Biocatalyst	Conversion (%)	ee Prod	Productivity <sup>c</sup>
N435 <sup>a</sup>	99	>99	0.17
EnzPd_1% <sup>b</sup>	84	>99	2.21
EnzPd_5% <sup>b</sup>	76	98	2.00
EnzPd_10% <sup>b</sup>	78	95	2.17
EnzNoPd <sup>a</sup>	92	82	2.36

<sup>a</sup> Reaction conditions: 5% of Pd supported on BaSO<sub>4</sub> as a racemization agent. A total of 3 mmol of  $\alpha$ -methylbenzylamine, 2 eq. of methyl methoxyacetate, biocatalyst (94 mg mmol<sup>-1</sup> of substrate), molecular sieves (30 mol%, 375 mg), Na<sub>2</sub>CO<sub>3</sub> (12 mg), 15 eq. of ammonium formate and toluene (3 mL) at 70 °C for 17 h, according to [112]. <sup>b</sup> Reaction conditions: 3 mmol of  $\alpha$ -methylbenzylamine; 2 eq. of methyl methoxyacetate, biocatalyst (94 mg mmol<sup>-1</sup> of substrate); molecular sieves (30 mol%, 375 mg); Na<sub>2</sub>CO<sub>3</sub> (12 mg); 15 eq. of ammonium formate and toluene (3 mL) at 70 °C for 17 h; <sup>c</sup> expressed on mg of product h<sup>-1</sup>. mg of immobilized enzyme<sup>-1</sup>.

In this work, lipase CaLB was immobilized on functionalized Pd-SiO<sub>2</sub> nanoparticles containing Pd in order to simplify the DKR of  $\alpha$ -methylbenzylamine. As a result, ee >99% and conversion of 82% were found, with only 1% of Pd, generating a productivity of 2.21 mg of product h<sup>-1</sup> mg of support<sup>-1</sup> against 0.76 found for N435<sup>®</sup>. Compared to commercial N435<sup>®</sup>, the novel biocatalysts showed protein loads about 15-fold lower and higher activity, demonstrating competitive performances and good industrial applications [111].

The biggest challenge in hybrid catalysis is to combine the best conditions of each system. The hybrid catalyst was around 50–100 nm with nanoparticulated Pd (5–10 nm) on its surface, and presented a superparamagnetic behavior without magnetization and 22 emu g<sup>-1</sup> of saturation magnetization [112]. As a result, it was possible to achieve a 99% conversion, with 95% selectivity and 93% enantiomeric excess after 12 h in batch. For a continuous flow system, it was possible to achieve a 95% conversion, with 71% selectivity and an ee > 99% after 60 min of reaction. Because the fixed-bed reactor system is pressurized, ammonium formate was used in this work as an in situ hydrogen source (Table 5) [112].

**Table 5.** DKR of biocatalysts using ammonium formate in continuous-flow condition [112].

Entry	Catalyst (Pd + CALB <sub>imm</sub> )	Reaction Time (h)	Conversion (%)	ee Prod (%)	Selectivity(%)
1	MN@4.5%Pd <sup>a</sup> + MN@CALB	1	95	>99	91
2	MN@4.5%Pd + N435 <sup>b</sup>	4	>99	>99	96
3	Pd/BaSO <sub>4</sub> + MN@CALB	1	65	>99	84
4	Pd/BaSO <sub>4</sub> + N435	1	72	97	94
5	MN@4.5%Pd_CALB	9	65	>99	88

<sup>a</sup> MN@4.5%Pd = Magnetic nanoparticle with 4.5% palladium; MN@ = hybrid catalyst without enzyme;

<sup>b</sup> N435 = Novozym<sup>®</sup> 435 (Lipase B de *Candida antarctica* immobilized) commercial; Pd/BaSO<sub>4</sub> = palladium immobilized on barium sulphate (commercial) and MN@4.5%Pd\_CALB = optimized hybrid catalyst.

As a result, a magnetic hybrid biocatalyst was able to promote high conversions and selectivities, close to systems where commercial lipase N435 was used as the enzyme source. Thus, the newly constructed hybrid biocatalyst becomes an interesting and robust alternative for obtaining chiral blocks containing amines [112].

We additionally developed two hybrid catalysis-based approaches to optimize the conversion reaction of d-glucose to 5-hydroxymethylfurfural (HMF). HMF is a platform molecule [113] opening the way to the synthesis of many compounds with applications in the fields of biofuels, biopolymers and a whole range of fine chemicals, making it one of the most studied platform molecules. To obtain HMF from d-glucose, the latter must first be isomerized to d-fructose. However, this reaction suffers from an unfavorable thermodynamic equilibrium which results in the presence of both sugars in almost equal quantities. An effective strategy consists of carrying out the isomerization with the aid of an enzyme and a d-glucose isomerase, and coupling this to the chemical dehydration step, making it

possible to achieve reaction equilibrium using a hybrid catalytic process. Several attempts have already been made in this respect, and we present below two of our developments using hybrid catalysis, one involving a classical enzymatic isomerization step coupled with an innovative compartmentalization approach to shift the equilibrium toward the products formation and an innovative hybrid isomerization step based on the combination of another enzyme and a chemo-catalyst for the regeneration of its co-substrate.

### 2.6.2. Compartmentalization

The compartmentalization based on the cascade reaction was the first approach studied in our laboratory [114–116]. This method is based on the subsequent dehydration of D-fructose to HMF using a Brønsted acid catalyst (as for example organic resin). These acid resins lead to a low pH value which is not appropriate for the isomerase enzyme. It is thus necessary to use a liquid membrane linking both compartments, which allows us to perform two sequential reactions of isomerization and dehydration without a cross-limitation between them. However, two main obstacles must be overcome: (i) the thermodynamic equilibrium of the enzymatic isomerization, and (ii) the incompatibility of the pH of the reaction for two catalysts. A methyl isobutyl ketone (MIBC) membrane was chosen in this study, allowing the fructose extraction from the aqueous “donor” phase (Figure 16). D-glucose isomerization was performed at pH = 8 using glucose isomerase. To achieve an efficient transfer through the membrane at room temperature, boronic acid derivatives were used in order to complex the formed fructose at the interface with the “donor” phase. Thanks to Aliquat336<sup>®</sup>, a quaternary amine, an ion pair was formed between the ester with a negatively charged 3,4-dichlorophenylboronic acid (3,4-DCPBA) and fructose [115,116]. Complexed fructose was then transformed to the “receiver” phase containing sulfonic resins, a dehydration catalyst. At pH 3, the fructose complex is hydrolyzed and d-fructose is dehydrated to HMF. An “H” type reactor was implemented, which permitted a better homogenization capacity of the phases. Fructose diffusion was also improved. After 32 h of reaction at a regulated pH (at 8.5 and 3.0) at 70 °C, the extraction yield was 97%. The isomerization yield reached 79% and the HMF yield reached 31% after 32 h of reaction (a glucose conversion of 88%) [115,116].

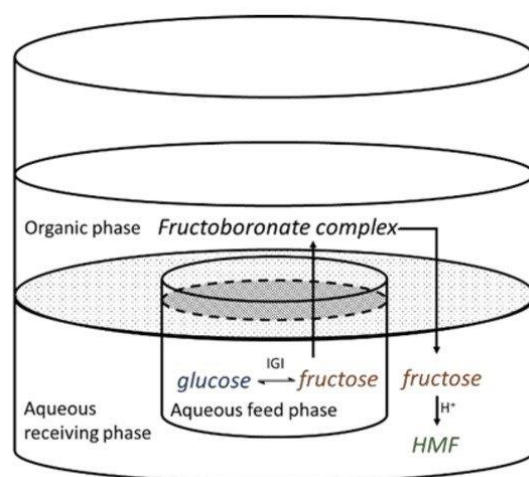


**Figure 16.** Concept of the compartmented sequential reactor with an organic solvent as the liquid membrane [116].

### 2.6.3. Hybrid Isomerization

Another studied variant was based on an innovative enzymatic cascade process. d-glucose is firstly hydrogenated to d-sorbitol, which is then selectively dehydrogenated to d-fructose. It must be noted, however, that the sorbitol dehydrogenase enzyme is NAD<sup>+</sup> dependent. The co-substrate must be regenerated throughout the reaction from the NADH formed. This step was carried out using an organometallic Ir-based catalyst (Figure 17).

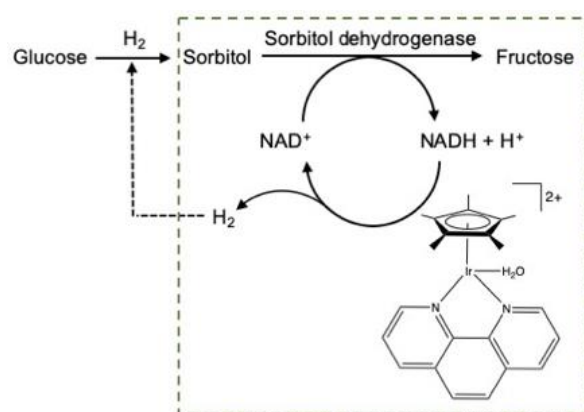


**Figure 17.** General concept of hybrid catalytic conversion of d-glucose into d-fructose using an iridium complex for NAD<sup>+</sup> regeneration.

We demonstrated the compatibility between the enzyme and a chemical catalyst (iridium complex) capable of in situ cofactor regeneration. This proof of concept was patented [114] and the results were published [115]. In addition, the catalyst based on Ir does not seem to constitute a “poison” for the enzyme. We have demonstrated, unambiguously, the continuous catalytic process of the complete system (substrate + cofactor + enzyme + organometallic complex). Up to now, three consecutive catalytic cycles of regeneration of the cofactor with the production of the target molecule were performed. The main challenges of the process concern the optimal operating pH values for both systems that are not compatible yet.

The one-pot approach, which can be described as “true hybrid catalysis”, effectively combines several catalysts within the same reactor, working together in the same conditions. In this way, the various substrates and intermediates are continuously converted as soon as they appear, which can make it possible to shift equilibria, limit inhibitions and thus considerably increase the activities of the catalysts. Recently, we have published an example of the use of hybrid catalysis for the transformation of biomass compounds [117]. This first study of its kind produced a new range of furfurylamines, with a special focus onto 5-aminofuran-2-carboxylic acid (AMFC), directly from HMF (Figure 18). To achieve such a process, for the first time ever reported, a transaminase was coupled with a heterogeneous chemo-catalyst, a platinum nanoparticle immobilized onto silica in this case.

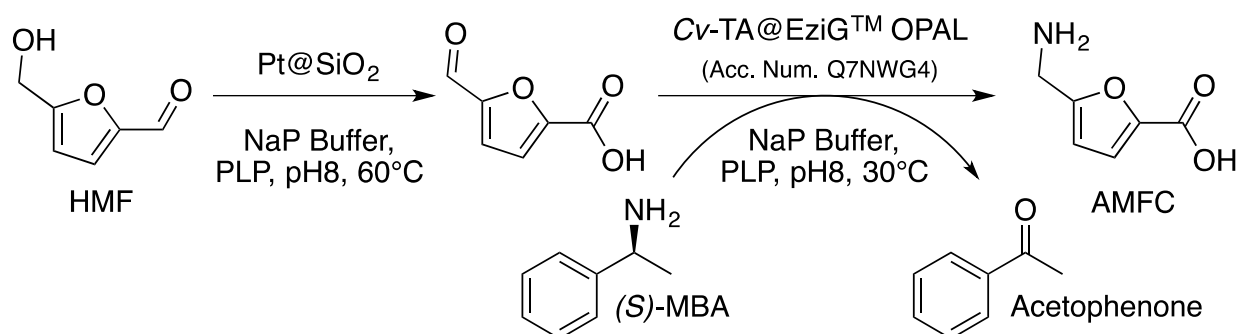


**Figure 18.** One-pot/two-step hybrid heterogeneous catalytic process for the conversion of HMF into AMFC, combining a Pt/SiO<sub>2</sub> chemocatalyst and the Cv-TA. Adapted with permission from Ref. [117].

By using a one-pot/two-step process, in which the enzyme was added directly to the reaction medium after the catalyst has completed its reaction and the temperature has dropped to around 30 °C, a 77% yield of FMCA can be achieved. It is noteworthy that the reaction medium was found to be compatible with both catalysts after its optimization

and that the only byproduct formed was 2,5-furandicarboxylic acid (FDCA; 23% yield obtained), a highly valuable monomer involved in polyethylene furanoate (PEF) synthesis.

### 2.7. Solving the Contextual Problem of Implementing Solutions

The contributions to this journal concern technical solutions to systemic problems: climate change, pollution, meeting the energy requirements of society, satisfying the market, the conversion of waste into a product to make the economy more circular, or the biodegradation of waste, the development of more refined and tailored materials to meet changing needs in society. The solutions are chemical or biochemical processes. They are innovative, scientifically interesting, if not ground-breaking, and relevant to addressing the systemic problems we face [3].

However, every technical solution, when implemented at the industrial scale, and over enough time, will meet a threshold with regard to causing more harm than good, in the way that we need salt in our bodies, but too much will kill you. In the age of the Anthropocene, we can no longer permit ourselves to implement solutions, at any scale and over any timeframe, that are only determined by demand and the profit of industry [3].

To determine the thresholds, we need to study the context for implementation. The context includes economics, but also society (health, politics, education, workforce, infrastructure, cultural values and security) and the ecology of the location of production, of distribution and of consumption, and then waste disposal. To study all of these elements is complicated. Worse, we cannot afford any longer to let the market work as a massive experiment where we learn through trial and error. As a society, we will have to make compromises and trade-offs. The task of determining what the trade-offs are and how to compare them is necessary, that is, to determine what solutions are worth pursuing and which seem impossible. Additionally, it is with the existing tools that we have: cost-benefit analysis, life-cycle analysis, material and energy flow models, multi-criteria decision aides, environmental impact assessments, cradle to grave analyses. However, these very difficult questions can be answered using an institutional compass [3].

To make a compass, we gather data about the technological solution process—mainly the input, output and distribution—on economic, social and environmental (entropy, pollution, disease, biodiversity . . . ) levels. We gather data for the proposed region of production, again at the economic, social and environmental levels. We analyze the data categorically along two axes—economics, society or environment—leading towards harmony, and discipline of excitement. The last three are general qualities. Upon reflection, we notice that any object or process will have one that predominates. *Prima facie*, none is better or worse, although we might have preferences for cultural or other reasons. Our preferred quality-place on the compass is called a wish-spot (Figure 19). We are not thinking in terms of a scale, but in terms simply of the qualities. The wish spot tells of our preference [3].

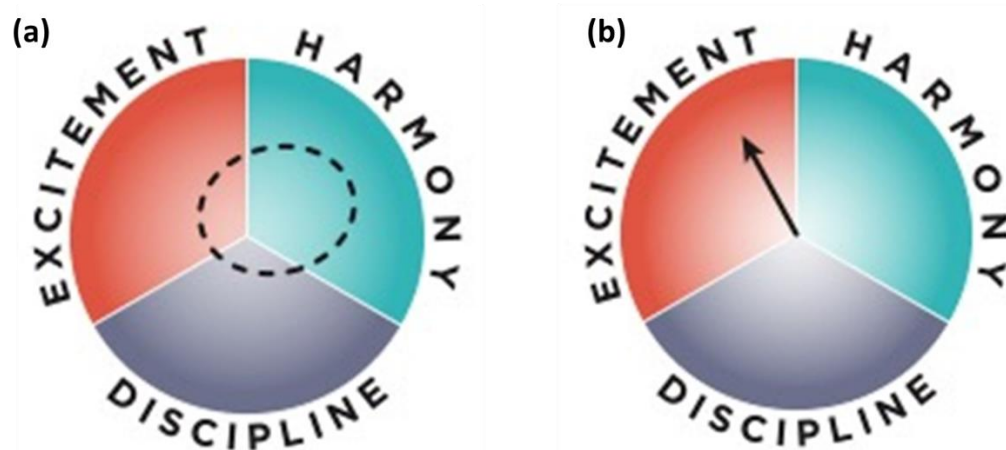


Figure 19. Comparing the wish spot (a) with the actual compass reading (b).

We then make a further, more refined analysis of each data point that is not involved in the technological solution. We analyze each data point in terms of the angle range within the quality “sector”. This is sensitive work, especially with the social data. There are straightforward methods for the economic and environmental data. We also determine a length of each data point scaled to the radius of the circle to indicate the importance, weight or momentum of the data point. The latter is achieved simply by determining the relative maximum and minimum values. We apply an algorithm that amalgamates all of the data to represent the whole as an arrow on the compass. This represents the general context for the production of the technological solution. We conduct a similar analysis at different scales for the data concerning the biochemical processes, and superimpose them, at different scales on the “general context of production” compass, to see how it fits in to the general context, and more importantly whether it brings the context arrow closer to the wish spot. We can thereby compare different contexts for their suitability at different scales for the proposed solution. We can compare different solutions to each other, for example, making biofuel from human-edible sugar plants or from farm-animal waste. We achieve this holistically and comprehensively, with a sensitivity to cultural values and expectations [3].

It is a shame to misuse the brilliant solutions brought to us by scientific research. It only benefits the discoveries and adds prestige to science when they are implemented responsively by our industrial partners. Thankfully, we can now ensure this better than we could before.

### 3. Discussion

The bioeconomy is a key parameter not only of the French but also of the whole European economy. A turnover value of EUR 2.3 trillion makes the European union (EU) a world leader in the sustainable use of the biobased resources [118]. A sustainable European bioeconomy supports the creation of new bio-based value chains and greener, more cost-effective industrial processes. Research and innovation in the field of new and sustainable bio-based products (biochemicals and biofuels) improve the European capacity to substitute fossil resources. It must be underlined that the sustainable bioeconomy is only a piece of the circular economy. In addition, there is not one single bioeconomy in Europe but several bioeconomies, each with specific local contexts. The chemical industry will be a key player in the European economy. It will allow residues and biowastes to be turned into valuable products which already creates new jobs in the markets of bio-based chemicals, pharmaceuticals and bio-based plastics production, while the employment in the classical fuel sectors decreased. This clearly shows that the use of biomass to produce highly added materials can directly increase employment by 10 times in Europe, and generate 4–9 times more added-value, compared to the current fossil-based economy [118]. As more than 90% of chemical processes are carried out using at least one catalyst (chemical, enzymatic, or heterogeneous), catalysis is in the very heart of the whole chemical industry.

In this context, the research projects developed in the VAALBIO group at UCCS encompass several key directions: biomass fractionation, cellulose [119,120] and hemicellulose valorization [121], green hydrogen production and CO<sub>2</sub> valorization [122–127], and more recently, multicyclic materials [128] and lignin valorization. As shown above, our research projects concern mainly the synthesis of important chemical synthons using heterogeneous and chemo-enzymatic processes. Some of these synthons are highly valued platform molecules that are building blocks for polymers or pharmaceutical complex molecules. It is worth adding that more than half of the projects are developed in collaboration with industrial partners which clearly makes the VAALBIO group an applied catalysis laboratory. The development of a circular economy also affects our research project's development. Recently, the VAALBIO group was awarded with a RECABIO “Catalyses and bioeconomy” flagship project from I-SITE ULNE [129]. The RECABIO project is a part of the development of innovative approaches in the field of bioeconomy, and more precisely in the circular economy. It aims at the use of advanced catalytic processes as an alternative to the transformation of renewable resources

and wastes to high-added-value molecules, materials and energy carriers. It implements original scientific approaches (in particular, hybrid catalysis, photo- and electro-catalysis as well as their combinations) thanks to (i) the advanced integration of a set of cutting-edge skills from the Lille site, (ii) the use of unique equipment with which our site is equipped (such as the REALCAT platform [130]), and (iii) the hosting of four recognized professors in the field of heterogenous and enzymatic catalysis, human sciences and LCA. The socio-economic and environmental rationalization of the processes thus developed must also be evaluated thanks to the close collaboration between the so-called “hard” sciences and the social sciences (LCA, economics, etc.). In this context, the reception of professors from different fields of science will support these topics, especially with regard to interconnected aspects. This convergence will allow new breakthrough discoveries and will induce an evolution of the concept of bioeconomy from a simple juxtaposition of disciplines (a necessary step that is currently well advanced) to a true integration of scientific and technical disciplines. To achieve this, the present project relies on interdisciplinary research efforts in the hard sciences aiming at lifting the scientific and societal barriers of the bioeconomy, and at questioning the consequences of the ecological mutation and its ethical, socio-political and socio-economic aspects. The ultimate ambition is to create new disciplines as a result of these interfaces, with a view to a global R&D approach, where production systems will be set in their social, political and environmental contexts.

#### 4. Conclusions

Catalytic processes are at the heart of chemical transformations. As the VAALBIO team, we study various catalytic processes. We are particularly well known for our work in the field of catalytic valorization of bio-based compounds, but we also have historical expertise in the valorization of light hydrocarbons (and more specifically alkanes) such as methane. These scientific themes, in full expansion, meet the needs of the chemical and energy sectors and will therefore remain at the heart of our team’s concerns for the coming years. The VAALBIO team has skills in chemistry but also in chemical engineering, which allows us to consider the development, not only of innovative catalysts, but also more broadly of catalytic processes as a whole, which constitute a real engine of innovation for the industry of tomorrow. In line with this dynamic, our projects keep a good balance between applied research (mainly supported by industrial partners) and fundamental research (generally supported by institutions). We are also developing an integrated approach to conduct catalytic processes, including the development of innovative contact modes and corresponding catalytic materials as well as processes combining several catalytic functions (hybrid catalysis). Furthermore, very recently, we included the “social” dimension to our project collaborating with experts in human sciences.

**Author Contributions:** All authors (M.A.-M., F.B.N., M.C., F.D., M.F., E.H., I.I.J., L.J.-D., A.L., B.K., S.P. and R.W.) contributed equally to this work. All authors have read and agreed to the published version of the manuscript.

**Funding:** This research received no external funding.

**Institutional Review Board Statement:** Not applicable.

**Informed Consent Statement:** Not applicable.

**Data Availability Statement:** Not applicable.

**Acknowledgments:** This study was supported by the French government through the Programme Investissement d’Avenir (I-SITE ULNE/ ANR-16-IDEX-0004 ULNE) managed by the Agence Nationale de la Recherche. Région Hauts de France (FEDER) and Métropole Européen de Lille (MEL) for “CatBioInnov” project are also acknowledged. Chevreul Institute (FR 2638), Ministère de l’Enseignement Supérieur, de la Recherche et de l’Innovation, Région Hauts de France are also acknowledged for supporting and partially funding this work.

**Conflicts of Interest:** The authors declare no conflict of interest.

## References

1. Dumeignil, F.; Capron, M.; Katryniok, B.; Wojcieszak, R.; Löfberg, A.; Girardon, J.S.; Desset, S.; Araque-Marin, M.; Jalowiecki-Duhamel, L.; Paul, S. Biomass-derived Platform Molecules Upgrading through Catalytic Processes: Yielding Chemicals and Fuels. *J. Jpn. Pet. Inst.* **2015**, *58*, 257–273. [[CrossRef](#)]
2. Heuson, E.; Froidevaux, R.; Itabaiiana, I., Jr.; Wojcieszak, R.; Capron, M.; Dumeignil, F. Optimisation of Catalysts Coupling in Multi-Catalytic Hybrid Materials: Perspectives for the Next Revolution in Catalysis. *Green Chem.* **2021**, *23*, 1942–1954. [[CrossRef](#)]
3. Friend, M. *The Institutional Compass: Method, Use and Scope*; Series: Methods; Springer Nature: Berlin, Germany, 2022; ISSN 2542-9892.
4. Kenar, J. Glycerol as a platform chemical: Sweet opportunities on the horizon? *Lipid Technol.* **2007**, *19*, 249–253. [[CrossRef](#)]
5. Katryniok, B.; Paul, S.; Capron, M.; Bellière-Baca, V.; Rey, P.; Dumeignil, F. Regeneration of Silica-Supported Silicotungstic Acid as a Catalyst for the Dehydration of Glycerol. *ChemSusChem* **2012**, *5*, 1298–1306. [[CrossRef](#)]
6. Skrzyńska, E.; Ftouni, J.; Girardon, J.S.; Capron, M.; Jalowiecki-Duhamel, L.; Paul, J.F.; Dumeignil, F. Quasi-Homogeneous Oxidation of Glycerol by Unsupported Gold Nanoparticles in the Liquid Phase. *ChemSusChem* **2012**, *5*, 2065–2068. [[CrossRef](#)] [[PubMed](#)]
7. Skrzyńska, E.; Ftouni, J.; Mamede, A.S.; Addad, A.; Trentesaux, M.; Girardon, J.S.; Capron, M.; Dumeignil, F. Glycerol oxidation over gold supported catalysts—“Two faces” of sulphur based anchoring agent. *J. Mol. Catal. A Chem.* **2014**, *382*, 71–78. [[CrossRef](#)]
8. Skrzyńska, E.; Zaid, S.; Girardon, J.S.; Capron, M.; Dumeignil, F. Catalytic behaviour of four different supported noble metals in the crude glycerol oxidation. *Appl. Catal. A Gen.* **2015**, *499*, 89–100. [[CrossRef](#)]
9. Dimitratos, N.; Villa, A.; Bianchi, C.L.; Prati, L.; Makkee, M. Gold on titania: Effect of preparation method in the liquid phase oxidation. *Appl. Catal. A Gen.* **2006**, *311*, 185. [[CrossRef](#)]
10. Díaz, J.A.; Skrzyńska, E.; Girardon, J.S.; Ftouni, J.; Capron, M.; Dumeignil, F.; Fongarland, P. Kinetic modeling of the quasi-homogeneous oxidation of glycerol over unsupported gold particles in the liquid phase. *Eur. J. Lipid Sci. Technol.* **2016**, *118*, 72–79. [[CrossRef](#)]
11. Díaz, J.A.; Skrzyńska, E.; Zaid, S.; Girardon, J.S.; Capron, M.; Dumeignil, F.; Fongarland, P. Kinetic modelling of the glycerol oxidation in the liquid phase: Comparison of Pt, Au and Ag As active phases. *J. Chem. Technol. Biotechnol.* **2017**, *92*, 2267–2275. [[CrossRef](#)]
12. Carrentin, S.; McMorn, P.; Johnston, P.; Griffin, K.; Hutchings, G. Selective oxidation of glycerol to glyceric acid using a gold catalyst in aqueous sodium hydroxide. *Chem. Commun.* **2002**, *7*, 696–697. [[CrossRef](#)] [[PubMed](#)]
13. Carrentin, S.; McMorn, P.; Johnston, P.; Griffin, K.; Kiely, J.; Hutchings, G. Oxidation of glycerol using supported Pt, Pd and Au catalysts. *Phys. Chem. Chem. Phys.* **2003**, *5*, 1329–1336. [[CrossRef](#)]
14. Li, Y.; Zaera, F. Sensitivity of the glycerol oxidation reaction to the size and shape of the platinum nanoparticles in Pt/SiO<sub>2</sub> catalysts. *J. Catal.* **2015**, *326*, 116. [[CrossRef](#)]
15. Skrzyńska, E.; El Roz, A.; Paul, S.; Capron, M.; Dumeignil, F. Glycerol Partial Oxidation over Pt/Al<sub>2</sub>O<sub>3</sub> Catalysts under Basic and Base-Free Conditions—Effect of the Particle Size. *J. Am. Oil Chem.* **2019**, *96*, 63–74. [[CrossRef](#)]
16. El Roz, A.; Fongarland, P.; Dumeignil, F.; Capron, M. Glycerol to Glyceraldehyde Oxidation Reaction Over Pt-Based Catalysts Under Base-Free Conditions. *Front. Chem.* **2019**, *7*, 156. [[CrossRef](#)] [[PubMed](#)]
17. Skrzyńska, E.; Zaid, S.; Addad, A.; Girardon, J.-S.; Capron, M.; Dumeignil, F. Performance of Ag/Al<sub>2</sub>O<sub>3</sub> catalysts in the liquid phase oxidation of glycerol—Effect of preparation method and reaction conditions. *Catal. Sci. Technol.* **2016**, *6*, 3182–3196. [[CrossRef](#)]
18. Zaid, S.; Skrzyńska, E.; Addad, A.; Nandi, S.; Jalowiecki-Duhamel, L.; Girardon, J.S.; Capron, M.; Dumeignil, F. Development of Silver Based Catalysts Promoted by Noble Metal M (M = Au, Pd or Pt) for Glycerol Oxidation in Liquid Phase. *Top. Catal.* **2017**, *60*, 1072–1081. [[CrossRef](#)]
19. Skrzyńska, E.; Capron, M.; Dumeignil, F.; Jalowiecki-Duhamel, L. Process for Preparing Glycolic Acid. WO Patent 2014/199256, 2014.
20. Tavera Ruiz, C.P.; Dumeignil, F.; Capron, M. Catalytic Production of Glycolic Acid from Glycerol Oxidation: An Optimization Using Response Surface Methodology. *Catalysts* **2021**, *11*, 257. [[CrossRef](#)]
21. Ishakawa, S.; Murayama, T.; Katryniok, B.; Dumeignil, F.; Araque, M.; Heyte, S.; Paul, S.; Yamada, Y.; Iwazaki, M.; Noda, N.; et al. Influence of the structure of trigonal Mo-V-M3rd oxides (M3rd = -, Fe, Cu, W) on catalytic performances in selective oxidations of ethane, acrolein, and allyl alcohol. *Appl. Catal. A Gen.* **2019**, *584*, 117151. [[CrossRef](#)]
22. Ishakawa, S.; Murayama, T.; Ohmura, S.; Sadakane, M.; Ueda, W. Synthesis of Novel Orthorhombic Mo and V Based Complex Oxides Coordinating Alkylammonium Cation in Its Heptagonal Channel and Their Application as a Catalyst. *Chem. Mater.* **2013**, *25*, 2211–2219. [[CrossRef](#)]
23. Chen, S.; Wojcieszak, R.; Dumeignil, F.; Marceau, E.; Royer, S. How Catalysts and Experimental Conditions Determine the Selective Hydroconversion of Furfural and 5-Hydroxymethylfurfural. *Chem. Rev.* **2018**, *118*, 11023–11117. [[CrossRef](#)] [[PubMed](#)]
24. Palombo Ferraz, C.; Navarro-Jaén, S.; Rossi, L.; Dumeignil, F.; Ghazzal, M.N.; Wojcieszak, R. Enhancing the activity of gold supported catalysts by oxide coating: Towards efficient oxidations. *Green Chem.* **2021**, *23*, 8453–8457. [[CrossRef](#)]
25. Al Rawas, H.; Palombo Ferraz, C.; Thuriot Roukos, J.; Heyte, S.; Paul, S.; Wojcieszak, R. Influence of Pd and Pt Promotion in Gold Based Bimetallic Catalysts on Selectivity Modulation in Furfural Base-Free Oxidation. *Catalysts* **2021**, *11*, 1226. [[CrossRef](#)]
26. Santarelli, F.; Paul, S.; Dumeignil, F.; Cavani, F.; Wojcieszak, R. Furoic Acid Preparation Method. WO Patent WO2017158106A1, 2017.

27. Roselli, A.; Carvalho, Y.; Dumeignil, F.; Cavani, F.; Paul, S.; Wojcieszak, R. Liquid Phase Furfural Oxidation under Uncontrolled pH in Batch and Flow Conditions: The Role of in Situ Formed Base. *Catalysts* **2020**, *10*, 73. [[CrossRef](#)]
28. Wojcieszak, R.; Palombo Ferraz, C.; Sha, J.; Houda, S.; Rossi, L.; Paul, S. Advances in Base-Free Oxidation of Bio-Based Compounds on Supported Gold Catalysts. *Catalysts* **2017**, *7*, 352. [[CrossRef](#)]
29. Palombo Ferraz, C.; Zieliński, M.; Pietrowski, M.; Heyte, S.; Dumeignil, F.; Rossi, L.; Wojcieszak, R. Influence of Support Basic Sites in Green Oxidation of Biobased Substrates Using Au-Promoted Catalysts. *ACS Sustain. Chem. Eng.* **2018**, *6*, 16332–16340. [[CrossRef](#)]
30. Palombo Ferraz, C.; Braga, A.; Ghazzal, N.; Zieliński, M.; Pietrowski, M.; Itabaiana, I., Jr.; Dumeignil, F.; Rossi, L.; Wojcieszak, R. Efficient Oxidative Esterification of Furfural Using Au Nanoparticles Supported on Group 2 Alkaline Earth Metal Oxides. *Catalysts* **2020**, *10*, 430. [[CrossRef](#)]
31. Palombo Ferraz, C.; da Silva Marques, A.; Rodrigues, T.; Camargo, P.; Paul, S.; Wojcieszak, R. Furfural Oxidation on Gold Supported on MnO<sub>2</sub>: Influence of the Support Structure on the Catalytic Performances. *Appl. Sci.* **2018**, *8*, 1246. [[CrossRef](#)]
32. da Silva Marques, A.; Rodrigues, T.; Candido, E.; de Freitas, I.; da Silva, A.; Fajardo, H.; Balzer, R.; Gomes, J.; Assaf, J.; de Oliveira, D.; et al. Combining active phase and support optimization in MnO<sub>2</sub>-Au nanoflowers: Enabling high activities towards green oxidations. *J. Coll. Interface Sci.* **2018**, *530*, 282–291. [[CrossRef](#)]
33. Palombo Ferraz, C.; Costa, N.; Teixeira-Neto, E.; Teixeira-Neto, A.; Liria, C.; Thuriot-Roukos, J.; Machini, T.; Froidevaux, R.; Dumeignil, F.; Rossi, L.; et al. 5-Hydroxymethylfurfural and Furfural Base-Free Oxidation over AuPd Embedded Bimetallic Nanoparticles. *Catalysts* **2020**, *10*, 75. [[CrossRef](#)]
34. Thuriot-Roukos, J.; Khadraoui, R.; Paul, S.; Wojcieszak, R. Raman Spectroscopy Applied to Monitor Furfural Liquid-Phase Oxidation Catalyzed by Supported Gold Nanoparticles. *ACS Omega* **2020**, *5*, 14283–14290. [[CrossRef](#)] [[PubMed](#)]
35. Fabien, D.; Snoussi, Y.; Itabaiana, I., Jr.; Wojcieszak, R. The Use of CO<sub>2</sub> in the Production of Bioplastics for an Even Greener Chemistry. *Sustainability* **2021**, *13*, 11278. [[CrossRef](#)]
36. Mazzi, A.; Paul, S.; Cavani, F.; Wojcieszak, R. Cyclohexane Oxidation to Adipic Acid Under Green Conditions: A Scalable and Sustainable Process. *ChemCatChem* **2018**, *10*, 3680–3682. [[CrossRef](#)]
37. Monti, E.; Ventimiglia, A.; Garcia Soto, C.A.; Martelli, F.; Rodríguez-Aguado, E.; Cecilia, J.A.; Sadier, A.; Ospitali, F.; Tabanelli, T.; Albonetti, S.; et al. Effect of the Colloidal Preparation Method for Supported Preformed Colloidal Au Nanoparticles for the Liquid Phase Oxidation of 1,6-Hexanediol to Adipic Acid. *Catalysts* **2022**, *12*, 196. [[CrossRef](#)]
38. Mattisson, T.; Keller, M.; Linderholm, C.; Moldenhauer, P.; Ryden, M.; Leion, H.; Lyngfelt, A. Chemical-looping technologies using circulating fluidized bed systems: Status of development. *Fuel Process. Technol.* **2018**, *172*, 1–12. [[CrossRef](#)]
39. Corma, A.; Sauvanaud, L. FCC testing at bench scale: New units, new processes, new feeds. *Catal. Today* **2013**, *218–219*, 107–114. [[CrossRef](#)]
40. Löfberg, A.; Guerrero-Caballero, J.; Kane, T.; Rubbens, A.; Jalowiecki-Duhamel, L. Ni/CeO<sub>2</sub> based catalysts as oxygen vectors for the chemical looping dry reforming of methane for syngas production. *Appl. Catal. B Environ.* **2017**, *212*, 159–174. [[CrossRef](#)]
41. Bhavsar, S.; Najera, M.; Vesper, G. Chemical Looping Dry Reforming as Novel, Intensified Process for CO<sub>2</sub> Activation. *Chem. Eng. Technol.* **2012**, *35*, 1281–1290. [[CrossRef](#)]
42. Löfberg, A.; Guerrero-Caballero, J. Plant and Process for Treating a Stream Comprising Hydrogen Sulfide. *WO Patent* **2016**.
43. Kalinkin, P.; Kovalenko, O.; Lapina, O.; Khabibulin, D.; Kundo, N. Kinetic peculiarities in the low-temperature oxidation of H<sub>2</sub>S over vanadium catalysts. *J. Mol. Catal. A Chem.* **2002**, *178*, 173–180. [[CrossRef](#)]
44. Kane, T.; Guerrero-Caballero, J.; Löfberg, A. H<sub>2</sub>S chemical looping selective and preferential oxidation to sulfur by bulk V<sub>2</sub>O<sub>5</sub>. *Appl. Catal. B Environ.* **2020**, *265*, 118566. [[CrossRef](#)]
45. Kane, T.; Guerrero-Caballero, J.; Löfberg, A. Chemical looping selective oxidation of H<sub>2</sub>S using V<sub>2</sub>O<sub>5</sub> impregnated over different supports as oxygen carriers. *ChemCatChem* **2020**, *12*, 2569–2579. [[CrossRef](#)]
46. Kane, T. Selective and Preferential Oxidation of Hydrogen Sulfide by Chemical Looping. Ph.D. Thesis, University of Lille, Lille, France, 4 December 2018.
47. de Souza, P.; Silvester, L.; da Silva, A.; Fernandes, C.; Rodrigues, T.; Paul, S.; Camargo, P.; Wojcieszak, R. Exploiting the Synergetic Behavior of PtPd Bimetallic Catalysts in the Selective Hydrogenation of Glucose and Furfural. *Catalysts* **2019**, *9*, 132. [[CrossRef](#)]
48. Silvester, L.; Ramos, F.; Thuriot-Roukos, J.; Heyte, S.; Araque, M.; Paul, S.; Wojcieszak, R. Fully integrated high-throughput methodology for the study of Ni- and Cu-supported catalysts for glucose hydrogenation. *Catal. Today* **2019**, *338*, 72–80. [[CrossRef](#)]
49. Sadier, A.; Shi, S.; Mamede, A.S.; Paul, S.; Marceau, E.; Wojcieszak, R. Selective aqueous phase hydrogenation of xylose to xylitol over SiO<sub>2</sub>-supported Ni and Ni-Fe catalysts: Benefits of promotion by Fe. *Appl. Catal. B Environ.* **2021**, *298*, 120564. [[CrossRef](#)]
50. Sadier, A.; Paul, S.; Marceau, E.; Wojcieszak, R. Ni-Fe alloying enhances the efficiency of the maltose hydrogenation process: The role of surface species and kinetic study. *Appl. Catal. B Environ.* **2022**, *313*, 121446. [[CrossRef](#)]
51. Dautzenberg, G.; Gerhardt, M.; Kamm, B. Bio based fuels and fuel additives from lignocellulose feedstock via the production of levulinic acid and furfural. *Holzforschung* **2011**, *65*, 439–451. [[CrossRef](#)]
52. Bu, Q.; Lei, H.; Zacher, A.H.; Wang, L.; Ren, S.; Liang, J.; Wei, Y.; Liu, Y.; Tang, J.; Zhang, Q.; et al. A review of catalytic hydrodeoxygenation of lignin-derived phenols from biomass pyrolysis. *Bioresour. Technol.* **2012**, *124*, 470–477. [[CrossRef](#)]
53. Besson, M.; Gallezot, P.; Pinel, C. Conversion of biomass into chemicals over metal catalysts. *Chem. Rev.* **2014**, *114*, 1827–1870. [[CrossRef](#)]

54. Lee, J.; Xu, Y.; Huber, G.W. High-throughput screening of monometallic catalysts for aqueous-phase hydrogenation of biomass-derived oxygenates. *Appl. Catal. B Environ.* **2013**, *140–141*, 98–107. [[CrossRef](#)]
55. Pizzi, R.; van Putten, R.-J.; Brust, H.; Perathoner, S.; Centi, G.; van der Waal, J.C. High-Throughput Screening of Heterogeneous Catalysts for the Conversion of Furfural to Bio-Based Fuel Components. *Catalysts* **2015**, *5*, 2244–2257. [[CrossRef](#)]
56. Alamillo, R.; Tucker, M.; Chia, M.; Pagañ-Torres, Y.; Dumesic, J. The selective hydrogenation of biomass-derived 5-hydroxymethylfurfural using heterogeneous catalysts. *Green Chem.* **2012**, *14*, 1413–1419. [[CrossRef](#)]
57. Shi, S.; Wojcieszak, R.; Paul, S.; Marceau, E. Ni Promotion by Fe: What Benefits for Catalytic Hydrogenation? *Catalysts* **2019**, *9*, 451. [[CrossRef](#)]
58. Shi, D.; Yang, Q.; Peterson, C.; Lamic-Humblot, A.F.; Girardon, J.S.; Griboval-Constant, A.; Stievano, L.; Sougrati, M.; Briois, V.; Bagot, P.; et al. Bimetallic Fe-Ni/SiO<sub>2</sub> catalysts for furfural hydrogenation: Identification of the interplay between Fe and Ni during deposition-precipitation and thermal treatments. *Catal. Today* **2019**, *334*, 162–172. [[CrossRef](#)]
59. Shi, D.; Sadier, A.; Girardon, J.S.; Mamede, A.S.; Ciotonea, C.; Marinova, M.; Stievano, L.; Sougrati, M.; La Fontaine, C.; Paul, S.; et al. Probing the core and surface composition of nanoalloy to rationalize its selectivity: Study of Ni-Fe/SiO<sub>2</sub> catalysts for liquid-phase hydrogenation. *Chem. Catal.* **2022**, *in press*. [[CrossRef](#)]
60. Chen, S.; Ciotonea, C.; De Oliveira Vigier, K.; François, J.; Wojcieszak, R.; Dumeignil, F.; Marceau, E.; Royer, S. Hydroconversion of 5-Hydroxymethylfurfural to 2,5-Dimethylfuran and 2,5-Dimethyltetrahydrofuran over Non-promoted Ni/SBA-15. *ChemCatChem* **2020**, *12*, 2050–2059. [[CrossRef](#)]
61. Katryniok, B.; Paul, S.; Bellière-Baca, V.; Rey, P.; Dumeignil, F. Glycerol Dehydration to Acrolein in the context of Glycerol new usages. *Green Chem.* **2010**, *12*, 2079–2098. [[CrossRef](#)]
62. Katryniok, B.; Kimura, H.; Skrzynska, E.; Girardon, J.S.; Fongerland, P.; Capron, M.; Ducoulombier, R.; Mimura, N.; Paul, S.; Dumeignil, F. Selective catalytic oxidation of glycerol: Perspectives for high value chemicals. *Green Chem.* **2011**, *13*, 1960–1979. [[CrossRef](#)]
63. Ebadipour, N.; Paul, S.; Katryniok, B.; Dumeignil, F. Alkaline-based catalysts for glycerol polymerization reaction: A review. *Catalysts* **2020**, *10*, 1021. [[CrossRef](#)]
64. Bouriakova, A.; Mendes, P.; Katryniok, B.; De Clercq, H.; Thybaut, J.W. Co-metal induced stabilization of alumina supported copper—Impact on in the hydrogenolysis of glycerol to 1,2-propanediol. *Catal. Commun.* **2020**, *164*, 106134. [[CrossRef](#)]
65. Tazawa, S.; Ota, N.; Tamura, M.; Nakagawa, Y.; Okumura, K.; Tomishige, K. Deoxydehydration with Molecular Hydrogen over Ceria-Supported Rhenium Catalyst with Gold Promoter. *ACS Catal.* **2016**, *6*, 6393–6397. [[CrossRef](#)]
66. Kon, Y.; Araque, M.; Nakashima, T.; Paul, S.; Dumeignil, F.; Katryniok, B. Direct Conversion of Glycerol to Allyl Alcohol over Alumina-supported Rhenium oxide. *Chem. Sel.* **2017**, *30*, 9864. [[CrossRef](#)]
67. Yi, J.; Liu, S.; Abu-Omar, M.M. Rhenium-catalyzed transfer hydrogenation and deoxygenation of biomass-derived polyols to small and useful organics. *ChemSusChem* **2012**, *5*, 1401–1404. [[CrossRef](#)] [[PubMed](#)]
68. Dethlefsen, J.R.; Lupp, D.; Oh, B.C.; Fristrup, P. Molybdenum-catalyzed deoxydehydration of vicinal diols. *ChemSusChem* **2014**, *7*, 425–428. [[CrossRef](#)]
69. Sandbrink, S.; Klindtworth, E.; Islam, H.U.; Beale, A.M.; Palkovits, R. ReOx/TiO<sub>2</sub>: A Recyclable Solid Catalyst for Deoxydehydration. *ACS Catal.* **2016**, *6*, 677–680. [[CrossRef](#)]
70. Silva, K.; Araque, M.; Katryniok, B. Production D'alcool Allylique à Partir de Glycérol en Phase Liquide. French Patent EP2021057525, 2021.
71. Kolbe, H.; Lautemann, E. Ueber die Constitution und Basicität der Salicylsäure. *Liebigs Ann. Chem.* **1860**, *115*, 157–206. [[CrossRef](#)]
72. Drault, F.; Snoussi, Y.; Paul, S.; Itabaiana, I.; Wojcieszak, R. Recent Advances in Carboxylation of Furoic Acid into 2,5-Furandicarboxylic Acid: Pathways towards Bio-Based Polymers. *ChemSusChem* **2020**, *13*, 5164–5172. [[CrossRef](#)]
73. Drault, F.; Snoussi, Y.; Thuriot-Roukos, J.; Paul, S.; Itabaiana, I.; Wojcieszak, R. Study of the Direct CO<sub>2</sub> Carboxylation Reaction on Supported Metal Nanoparticles. *Catalysts* **2021**, *11*, 326. [[CrossRef](#)]
74. Liebig, C.; Paul, S.; Katryniok, B.; Guillon, C.; Couturier, J.-L.; Dubois, J.-L.; Dumeignil, F.; Hölderich, W.F. Glycerol conversion to acrylonitrile by consecutive dehydration over WO<sub>3</sub>/TiO<sub>2</sub> and ammoxidation over Sb-/Fe,V-O. *Appl. Catal. B Environ.* **2013**, *132–133*, 170–182. [[CrossRef](#)]
75. Guillon, C.; Liebig, C.; Paul, S.; Mamede, A.-S.; Hölderich, W.F.; Dumeignil, F.; Katryniok, B. Ammoxidation of allyl alcohol—A sustainable route to acrylonitrile. *Green Chem.* **2013**, *13*, 3015–3019. [[CrossRef](#)]
76. Ebadi, N.; Dumeignil, F.; Katryniok, B.; Delevoeye, L.; Revel, B.; Paul, S. Investigating the active phase of Ca-based glycerol polymerization catalysts: On the importance of calcium glycerolate. *Mol. Catal.* **2021**, *507*, 111571. [[CrossRef](#)]
77. Pomalaza, G.; Capron, M.; Ordonsky, V.; Dumeignil, F. Recent Breakthroughs in the Conversion of Ethanol to Butadiene. *Catalysts* **2016**, *6*, 203. [[CrossRef](#)]
78. Pomalaza, G.; Arango, P.; Capron, M.; Dumeignil, F. Butadiene from Ethanol: The Reaction and its catalysts. *Catal. Sci. Technol.* **2020**, *10*, 4860–4911. [[CrossRef](#)]
79. Pomalaza, G.; Capron, M.; Dumeignil, F. Improving the Synthesis of Zn-Ta-TUD-1 for the Lebedev Process using the Design of Experiments Methodology. *Appl. Catal. A Gen.* **2020**, *591*, 117386. [[CrossRef](#)]
80. Pomalaza, G.; Capron, M.; Dumeignil, F. ZnTa-TUD-1 as Easily Prepared, Highly Efficient Catalyst for the Selective Conversion of Ethanol to 1,3-Butadiene. *Green Chem.* **2018**, *20*, 3203–3209. [[CrossRef](#)]

81. Pomalaza, G.; Simon, P.; Addad, A.; Capron, M.; Dumeignil, F. Properties and Activity of Zn-Ta-TUD-1 in the Lebedev Process. *Green Chem.* **2020**, *22*, 2558–2574. [[CrossRef](#)]
82. Duhamel, L.; Fang, W.; Paul, S.; Dumeignil, F. Process for Production of Hydrogen. U.S. Patent 9,968,913, 2018.
83. Pirez, C.; Fang, W.; Capron, M.; Paul, S.; Jobic, H.; Dumeignil, F.; Jalowiecki-Duhamel, L. Steam reforming, partial oxidation and oxidative steam reforming for hydrogen production from ethanol over cerium nickel based oxyhydride catalyst. *Appl. Catal. A Gen.* **2016**, *518*, 78–86. [[CrossRef](#)]
84. Fang, W.; Paul, S.; Capron, M.; Biradar, A.V.; Umbarkar, S.B.; Dongare, M.K.; Dumeignil, F.; Jalowiecki-Duhamel, L. Highly loaded well dispersed stable Ni species in Ni<sub>x</sub>Mg<sub>2</sub>AlO<sub>y</sub> nanocomposites: Application to hydrogen production from bioethanol. *Appl. Catal. B Environ.* **2015**, *166–167*, 485–496. [[CrossRef](#)]
85. Fang, W.; Pirez, C.; Paul, S.; Jiménez-Ruiz, M.; Jobic, H.H.; Dumeignil, F.; Jalowiecki-Duhamel, L. Advanced functionalized Mg<sub>2</sub>AlNi<sub>x</sub>H<sub>z</sub>O<sub>y</sub> nano-oxyhydrides ex-hydrotalcites for hydrogen production from oxidative steam reforming of ethanol. *Int. J. Hydr. Energy* **2016**, *41*, 15443–15452. [[CrossRef](#)]
86. Fang, W.; Romani, Y.; Wei, Y.; Jiménez-Ruiz, M.M.; Jobic, H.; Paul, S.; Jalowiecki-Duhamel, L. Steam reforming and oxidative steam reforming for hydrogen production from bioethanol over Mg<sub>2</sub>AlNi<sub>x</sub>H<sub>z</sub>O<sub>y</sub> nano-oxyhydride catalysts. *Int. J. Hydrogen Energy* **2018**, *43*, 17643–17655. [[CrossRef](#)]
87. Löfberg, A.; Kane, T.; Guerrero-Caballero, J.; Jalowiecki-Duhamel, L. Chemical looping dry reforming of methane: Towards shale-gas and biogas valorization. *Chem. Eng. Process. Process Intensif.* **2017**, *122*, 523–529. [[CrossRef](#)]
88. Guerrero-Caballero, J.; Kane, T.; Haidar, N.; Jalowiecki-Duhamel, L.; Löfberg, A. Ni, Co, Fe supported on Ceria and Zr doped Ceria as oxygen carriers for chemical looping dry reforming of methane. *Catal. Today* **2019**, *333*, 251–258. [[CrossRef](#)]
89. Wei, Y.; Liu, X.; Haidar, N.; Jobic, H.; Paul, S.; Jalowiecki-Duhamel, L. CeNi<sub>x</sub>Al<sub>0.5</sub>H<sub>z</sub>O<sub>y</sub> nano-oxyhydrides for H<sub>2</sub> production by oxidative dry reforming of CH<sub>4</sub> without carbon formation. *Appl. Catal. A Gen.* **2020**, *594*, 117439. [[CrossRef](#)]
90. Managutti, P.; Tymen, S.; Liu, X.; Hernandez, O.; Prestipino, C.; Le Gal La Salle, A.; Paul, S.; Jalowiecki-Duhamel, L.; Dorcet, V.; Billard, A.; et al. Exsolution of Ni nanoparticles from A-site deficient layered double perovskites for dry reforming of methane and as anode material for solid oxide fuel cell. *ACS Appl. Mater. Interfaces* **2021**, *13*, 35719–35728. [[CrossRef](#)] [[PubMed](#)]
91. Bi, Z.; Lai, B.; Zhao, Y.; Yan, L. Fast Disassembly of Lignocellulosic Biomass to Lignin and Sugars by Molten Salt Hydrate at Low Temperature for Overall Biorefinery. *ACS Omega* **2018**, *3*, 2984–2993. [[CrossRef](#)]
92. Leipner, H.; Fischer, S.; Brendler, E.; Voigt, W. Structural changes of cellulose dissolved in molten salt hydrates. *Macromol. Chem. Phys.* **2000**, *201*, 2041–2049. [[CrossRef](#)]
93. Sen, S.; Losey, B.P.; Gordon, E.E.; Argyropoulos, D.S.; Martin, J.D. Ionic Liquid Character of Zinc Chloride Hydrates Define Solvent Characteristics that Afford the Solubility of Cellulose. *J. Phys. Chem. B* **2016**, *120*, 1134–1141. [[CrossRef](#)]
94. Quiroz, N.R.; Padmanathan, A.M.D.; Mushrif, S.H.; Vlachos, D.G. Understanding Acidity of Molten Salt Hydrate Media for Cellulose Hydrolysis by Combining Kinetic Studies, Electrolyte Solution Modeling, Molecular Dynamics Simulations, and <sup>13</sup>C NMR Experiments. *ACS Catal.* **2019**, *9*, 10551–10561. [[CrossRef](#)]
95. Sen, S.; Martin, J.D.; Argyropoulos, D.S. Review of Cellulose Non-Derivatizing Solvent Interactions with Emphasis on Activity in Inorganic Molten Salt Hydrates. *ACS Sustain. Chem. Eng.* **2013**, *1*, 858–870. [[CrossRef](#)]
96. Ragg, P.L.; Fields, P.R. The development of a process for the hydrolysis of lignocellulosic waste. *Phil. Trans. R. Soc. Land. A* **1987**, *321*, 537–547. [[CrossRef](#)]
97. Fischer, S.; Leipner, H.; Thümmel, K.; Brendler, E.; Peters, J. Inorganic Molten Salts as Solvents for Cellulose. *Cellulose* **2003**, *10*, 227–236. [[CrossRef](#)]
98. Deng, W.; Kennedy, J.R.; Tsilomelekis, G.; Zheng, W.; Nikolakis, V. Cellulose Hydrolysis in Acidified LiBr Molten Salt Hydrate Media. *Ind. Eng. Chem. Res.* **2015**, *54*, 5226–5236. [[CrossRef](#)]
99. Liu, Q.; Ma, Q.; Sabnis, S.; Zheng, W.; Vlachos, D.G.; Fan, W.; Li, W.; Ma, L. Production of high-yield short-chain oligomers from cellulose via selective hydrolysis in molten salt hydrates and separation. *Green Chem.* **2019**, *21*, 5030–5038. [[CrossRef](#)]
100. Ahmed, S.T.; Leferink, N.; Scrutton, N. Chemo-enzymatic routes towards the synthesis of bio-based monomers and polymers. *Mol. Catal.* **2019**, *467*, 95–110. [[CrossRef](#)]
101. Wojcieszak, R.; Itabaiana, I., Jr. Engineering the future: Perspectives in the 2,5-furandicarboxylic acid synthesis. *Catal. Today* **2020**, *354*, 211–217. [[CrossRef](#)]
102. Dumeignil, F. Hailing the hybrid—Professor Franck Dumeignil, EuroBioref Coordinator at the Université Lille Nord de France turns the spotlight onto a new golden age of catalysis. *Public Serv. Rev. Eur. Union* **2011**, *22*, 528.
103. Dumeignil, F. Chemical Catalysis and Biotechnology: From a Sequential Engagement to a One-Pot Wedding. *Chem. Ing. Tech.* **2014**, *86*, 1496. [[CrossRef](#)]
104. Dumeignil, F.; Guehl, M.; Gimbernat, A.; Capron, M.; Lopes Ferreira, N.; Froidevaux, R.; Girardon, J.S.; Wojcieszak, R.; Dhulster, P.; Delcroix, D. From Sequential Chemoenzymatic Synthesis to Integrated Hybrid Catalysis: Taking the Best of Both Worlds to Open up the Scope of Possibilities for a Sustainable Future. *Catal. Sci. Technol.* **2018**, *8*, 5708–5734. [[CrossRef](#)]
105. Heuson, E.; Dumeignil, F. The Various Levels of Integration of Chemo- and Bio-Catalysis towards Hybrid Catalysis. *Catal. Sci. Technol.* **2020**, *12*, 7082–7100. [[CrossRef](#)]
106. Lee, J.H.; Han, K.; Kim, M.-J.; Park, J. Chemoenzymatic dynamic kinetic resolution of alcohols and amines. *Eur. J. Org. Chem.* **2010**, *6*, 999–1015. [[CrossRef](#)]

107. Kamal, A.; Azhar, M.A.; Krishnaji, T.; Malik, M.S.; Azeeda, S. Approaches based on enzyme mediated kinetic to dynamic kinetic resolutions: A versatile route for chiral intermediates. *Coord. Chem. Rev.* **2008**, *252*, 569–592. [CrossRef]
108. De Miranda, A.S.; De Souza, L.; de Souza, R.O.M.A. Lipases: Valuable catalysts for dynamic kinetic resolutions. *Biotechnol. Adv.* **2015**, *33*, 372–393. [CrossRef] [PubMed]
109. Ghislieri, D.; Turner, N. Biocatalytic Approaches to the Synthesis of Enantiomerically Pure Chiral Amines. *Top. Catal.* **2014**, *57*, 284–300. [CrossRef]
110. Itabaiana, I., Jr.; Miranda, L.; de Souza, R. Towards a continuous flow environment for lipase-catalyzed reactions. *J. Mol. Catal. B Enzym.* **2013**, *85–86*, 1–9. [CrossRef]
111. de Souza, S.; Leão, R.; Bassut, J.; Leal, I.; Wang, S.; Ding, Q.; Li, Y.; Leung-Yuk Lam, F.; de Souza, R.; Itabaiana, I., Jr. New Biosilified Pd-lipase hybrid biocatalysts for dynamic resolution of amines. *Tetrahedron Lett.* **2017**, *58*, 4849–4854. [CrossRef]
112. Ferraz, C.; do Nascimento, M.; Almeida, R.; Sergio, G.; Junior, A.; Dalmônico, G.; Caraballo, R.; Finotelli, P.; Leão, R.; Wojcieszak, R.; et al. Synthesis and characterization of a magnetic hybrid catalyst containing lipase and palladium and its application on the dynamic kinetic resolution of amines. *Mol. Catal.* **2020**, *493*, 111106. [CrossRef]
113. van Putten, R.; van der Waal, J.; de Jong, E.; Rasrendra, C.; Heeres, H.; de Vries, J. Hydroxymethylfurfural, A Versatile Platform Chemical Made from Renewable Resources. *Chem. Rev.* **2013**, *113*, 1499–1597. [CrossRef]
114. Guehl, M.; Delcroix, D.; Lopes Ferreira, N.; Desset, S.; Dumeignil, F. Process for the selective transformation of biosourced polyols. FR Patent FR3031983A1, 2016.
115. Gimbernat, A.; Guehl, M.; Capron, M.; Lopes Ferreira, N.; Froidevaux, R.; Girardon, J.S.; Dhulster, P.; Delcroix, D.; Dumeignil, F. Hybrid Catalysis: A Suitable Concept for the Valorization of Biosourced Saccharides to Value-Added Chemicals. *ChemCatChem* **2017**, *9*, 2080–2084. [CrossRef]
116. Gimbernat, A.; Guehl, M.; Lopes Ferreira, N.; Heuson, E.; Dhulster, P.; Capron, M.; Dumeignil, F.; Delcroix, D.; Girardon, J.S.; Froidevaux, R. From a Sequential Chemo-Enzymatic Approach to a Continuous Process for HMF Production from Glucose. *Catalysts* **2018**, *8*, 335. [CrossRef]
117. Lancien, A.; Wojcieszak, R.; Cuvelier, E.; Duban, M.; Dhulster, P.; Paul, S.; Dumeignil, F.; Froidevaux, R.; Heuson, E. Hybrid Conversion of 5-Hydroxymethylfurfural to 5-Aminomethyl-2-furancarboxylic acid: Toward New Bio-sourced Polymers. *ChemCatChem* **2021**, *13*, 247–259. [CrossRef]
118. EU Bioeconomy Strategy. A Sustainable Bioeconomy for Europe: Strengthening the Connection Between Economy, Society and the Environment, European Commission B-1049, Brussels, 2018. Available online: <https://eur-lex.europa.eu/legal-content/en/ALL/?uri=CELEX%3A52018DC0673> (accessed on 20 May 2022).
119. Avelar do Nascimento, M.; Ester Gotardo, L.; Míguez Bastos, E.; Almeida, F.; Leão, R.; Wojcieszak, R.; Itabaiana, I., Jr.; de Souza, R. Regioselective Acylation of Levoglucosan Catalyzed by Candida Antarctica (CaLB) Lipase Immobilized on Epoxy Resin. *Sustainability* **2019**, *11*, 6044. [CrossRef]
120. Itabaiana Junior, I.; Avelar do Nascimento, A.; de Souza, R.; Dufour, D.; Wojcieszak, R. Levoglucosan: A promising platform molecule? *Green Chem.* **2020**, *22*, 5859–5880. [CrossRef]
121. Wojcieszak, R.; Santarelli, F.; Paul, S.; Dumeignil, F.; Cavani, F.; Gonçalves, R. Recent developments in maleic acid synthesis from bio-based chemicals. *Sustain. Chem. Proc.* **2015**, *3*, 9. [CrossRef]
122. Gonçalves Renato, V.; Vono, L.; Wojcieszak, R.; Dias, C.; Wender, H.; Teixeira-Neto, E.; Rossi, L. Selective hydrogenation of CO<sub>2</sub> into CO on a highly dispersed nickel catalyst obtained by magnetron sputtering deposition: A step towards liquid fuels. *Appl. Catal. B Environ.* **2017**, *209*, 240–246. [CrossRef]
123. Navarro-Jaén, S.; Bonin, J.V.; Robert, M.; Wojcieszak, R.; Khodakov, A. Highlights and challenges in the selective reduction of carbon dioxide to methanol. *Nat. Rev. Chem.* **2021**, *5*, 564–579. [CrossRef]
124. Navarro-Jaén, S.; Morin, J.C.V.; Thuriot-Roukos, J.; Wojcieszak, R.; Khodakov, A. Hybrid monometallic and bimetallic copper-palladium zeolite catalysts for direct synthesis of dimethyl ether from CO<sub>2</sub>. *New J. Chem.* **2022**, *46*, 3889–3900. [CrossRef]
125. Navarro-Jaén, S.; Virginie, M.; Thuriot-Roukos, J.; Wojcieszak, R.; Khodakov, A. Structure–performance correlations in the hybrid oxide-supported copper–zinc SAPO-34 catalysts for direct synthesis of dimethyl ether from CO<sub>2</sub>. *J. Mater. Sci.* **2022**, *57*, 3268–3279. [CrossRef]
126. Barrios, A.; Peron, D.; Chakkingal, A.; Dugulan, A.J.; Moldovan, S.; Nakouri, K.; Thuriot-Roukos, J.; Wojcieszak, R.; Thybaut, J.; Virginie, M.; et al. Efficient Promoters and Reaction Paths in the CO<sub>2</sub> Hydrogenation to Light Olefins over Zirconia-Supported Iron Catalysts. *ACS Catal.* **2022**, *12*, 3211–3225. [CrossRef]
127. Shi, D.; Heyte, S.; Capron, M.; Paul, S. Catalytic processes for the direct synthesis of dimethyl carbonate from CO<sub>2</sub> and methanol: A review. *Green Chem.* **2022**, *24*, 1067–1089. [CrossRef]
128. Júnior, A.A.d.T.; da Silva França, A.; de Souza, R.O.M.A.; Henrique Moraes, A.; Wojcieszak, R.; Itabaiana, I., Jr.; de Miranda, A.S. Multicatalytic Hybrid Materials for Biocatalytic and Chemoenzymatic Cascades—Strategies for Multicatalyst (Enzyme) Co-Immobilization. *Catalysts* **2021**, *11*, 936. [CrossRef]
129. RECABIO. Available online: <http://www.isite-ulne.fr/index.php/fr/recabio/> (accessed on 22 May 2022).
130. REALCAT. Available online: <https://www.realcat.fr> (accessed on 22 May 2022).